5. Treatment of physical processes

5.1 Horizontal diffusion

Two types of diffusions are used to control nonlinear instability and aliasing. These are a second-order diffusion of the form

$$F_{H2\alpha} = p^* K_H \nabla_\sigma^2 \alpha, \tag{5.1.1}$$

where α is any prognostic variable, and a more scale-selective fourth-order form

$$F_{H4\alpha} = p^* K'_H \nabla_\sigma^4 \alpha, \tag{5.1.2}$$

where

$$K'_H = \Delta s^2 K_H \qquad (5.1.3),$$

The second order diffusion is only used in the coarsest domain for the row and column of the grid points next to the lateral boundaries, while the fourth-order form is used in the interior of the coarsest domain as well as in the entire domain of any refinement mesh.

The horizontal diffusion coefficient K_H consists of a background value K_{H0} and a term proportional to the deformation D

$$K_H = K_{H0} + .5k^2 \Delta s_2 D \tag{5.1.4}$$

where k is the von Karman constant and D is given by (Smagorinski *et al.* 1965)

$$D = \left[\left(\frac{\partial u}{\partial x} - \frac{\partial v}{\partial y} \right)^2 + \left(\frac{\partial v}{\partial x} + \frac{\partial u}{\partial y} \right)^2 \right]^{\frac{1}{2}}. \tag{5.1.5}$$

A background value of K_H is a function of grid size and time step, where

$$K_{H0} = 3. \times 10^{-3} \frac{\Delta x^2}{\Delta t}. \tag{5.1.6}$$

Note that the horizontal operators ∇^4 and ∇^2 are applied on constant sigma surfaces. To ensure computational stability, an upper limit of $\frac{\Delta x^2}{64 \Delta t}$ is imposed on K_H

5.2 Dry Convective Adjustment

There may be situations in which super-adiabatic layers are produced in the model atmosphere. When this happens, and there is no call to the Blackadar planetary boundary layer parameterization, a simple scheme is used to remove any unstable layers. The scheme operates on the entire sounding at once and conserves the vertical integral of internal and potential energy. When the model lapse rate of potential temperature $\frac{\partial\theta}{\partial p}$ exceeds a critical value $\left(\frac{\partial\theta}{\partial p}\right)_c$, the sounding is adjusted so that (1) mass-weighted mean temperature is unchanged, and (2) the potential temperature lapse rate after adjustment equals $\left(\frac{\partial\theta}{\partial p}\right)_c$.

Given n layers in which the model potential temperature lapse rate exceeds the critical value, the first constraint gives

$$(T_n + \Delta T_n)\Delta\sigma_n + (T_{n-1} + \Delta T_{n-1})\Delta\sigma_{n-1} + ... + (T_1 + \Delta T_1)\Delta\sigma_1 = \bar{T}\sum_{i-1}^{n}\Delta\sigma_i, \quad (5.2.1)$$

where T_i are the adjustments to be added to the temperature at layer i, T_i and σ_i are the temperature and thickness of the sigma layers, and $\bar{T}$ is the mass weighted mean temperature. The second constraint gives

$$(T_i + \Delta T_i)\pi_i - (T_{i-1} + \Delta T_{i-1})\pi_{i-1} = \left(\frac{\partial\theta}{\partial p}\right)(p_i - p_{i-1}) \qquad i = 2, ..., n, \qquad (5.2.2)$$

where π_i is the Exner function. There are n equations that can be solved for n variables ΔT_i. The Gaussian elimination method is used to solve the $n \times n$ matrix system. After adjustment, the entire sounding is rechecked for unstable layers.

The moisture in the adjusted layers is assumed constant in the vertical, i.e.,

$$q_{vi} = \bar{q_v} = \frac{\sum_{i=1}^{n} q_{vi}\Delta\sigma_i}{\sum_{i=1}^{n}\Delta\sigma_i} \qquad (5.1.3)$$

5.3 Precipitation physics

MM5 has many different choices to treat precipitation physics. They are usually divided into two different groups: explicit and implicit schemes. Explicit schemes treat resolved precipitation physics while implicit schemes treat the non-resolved precipitation physics. Both may be operating at a grid-point at the same time. A commonly used terminology of "convective" versus "stable" precipitation is generally not acceptable on finer grid-resolutions, where convective precipitation is quite often resolved. Hence in the following subsections we will use resolved/non-resolved and explicit/implicit as common terminologies. As two additional options, MM5 allows for dry runs, where moisture is treated as a passive variable (no explicit and implicit schemes are applied). Another option is a "fake dry run", where only the effects of the latent heat release are removed. These 2 options do not require any further description and will not be discussed in the following subsections.

5.3.1 Resolvable scale precipitation processes

These schemes are usually activated whenever grid-scale saturation is reached. In other words, they treat resolved precipitation processes. The most simple way that sometimes is still used on larger-scales, is to simply remove super-saturation as precipitation and add the latent heat to the thermodynamic equation. More sophisticated schemes carry additional variables such as cloud and rainwater (subsection 5.3.1.1), or even ice and snow (subsection 5.3.1.2). Both schemes described next are enhancements of MM4's original scheme (Hsie 1984).

5.3.1.1 Explicit treatment of cloudwater, rainwater, snow, and ice

This scheme optionally allows for ice-phase processes below 0 °C, where cloud water is treated as cloud ice and rain is treated as snow (Dudhia 1989). The equations for water vapor, cloud water (ice) and rain water (snow) mixing ratios are given by the following

$$\frac{\partial p^* q_v}{\partial t} = -m^2\left[\frac{\partial p^* u q_v/m}{\partial x} + \frac{\partial p^* v q_v/m}{\partial y}\right] - \frac{\partial p^* q_v \dot{\sigma}}{\partial \sigma} + \delta_{nh} q_v DIV$$

$$+ p^*(-P_{RE} - P_{CON} - P_{II} - P_{ID}) + D_{qv}, \tag{5.3.1.1.1}$$

$$\frac{\partial p^* q_c}{\partial t} = -m^2\left[\frac{\partial p^* u q_c/m}{\partial x} + \frac{\partial p^* v q_c/m}{\partial y}\right] - \frac{\partial p^* q_c \dot{\sigma}}{\partial \sigma} + \delta_{nh} q_c DIV$$

$$+ p^*(P_{ID} + P_{II} - P_{RC} - P_{RA} + P_{CON}) + D_{qc}, \tag{5.3.1.1.2}$$

$$\frac{\partial p^* q_r}{\partial t} = -m^2\left[\frac{\partial p^* u q_r/m}{\partial x} + \frac{\partial p^* v q_r/m}{\partial y}\right] - \frac{\partial p^* q_r \dot{\sigma}}{\partial \sigma} + \delta_{nh} q_r DIV$$

$$- \frac{\partial V_f \rho g q_r}{\partial \sigma} + p^*(P_{RE} + P_{RC} + P_{RA}) + D_{qr}, \tag{5.3.1.1.3}$$

where P_{CON} is condensation (and freezing for $T < 0$ °C) of water vapor into cloud (ice) at water saturation, P_{RA} is accretion of cloud by rain (ice by snow), P_{RC} is conversion of cloud to rain (ice to snow) and P_{RE} is evaporation (sublimation) of rain (snow). Additional ice processes are P_{II}, the initiation of ice crystals, and P_{ID} sublimation/deposition of cloud ice (Fig. 5.1). The fall speed of rain or snow is V_f. The term δ_{nh} is 1 for nonhydrostatic and 0 for hydrostatic simulations.

In all the relevant processes, Marshall-Palmer size distributions are assumed for rain and snow and droplet fall speeds are taken to be of the form $V(D) = aD^b$, where D is the diameter. For rain, the Marshall-Palmer intercept parameter is $N_0 = 8 \times 10^6$ m^{-4}, $a = 841.99667$ and $b = 0.8$ for V in m s^{-1}and D in meters, while for snow $N_0 = 2 \times 10^7$ m^{-4}, $a = 11.72$ and $b = 0.41$.

The saturated vapor pressure over water (in mb) is taken to be

$$e_{sw} = 6.112\exp\left[17.67\left(\frac{T - 273.15}{T - 29.65}\right)\right], \tag{5.3.1.1.4}$$

and for ice

$$e_{si} = 6.11\exp\left(22.514 - \frac{6150}{T}\right). \tag{5.3.1.1.5}$$

The saturated water vapor mixing ratio is then given by

$$q_s = \frac{0.622 e_s}{p - e_s}.$$

P_{RC}, the autoconversion term is represented by

$$P_{RC} = \max[k_1(q_c - q_{crit}),\ 0], \tag{5.3.1.1.6a}$$

for cloud to rain and by

$$P_{RC} = \max[(q_c - M_{max}n_c)/\Delta t,\ 0], \tag{5.3.1.1.6b}$$

for ice to snow, where $k_1 = 10^{-3}$ s^{-1}, $q_{crit} = 0.5$ g kg^{-1}, $M_{max} = 9.4 \times 10^{-10}$ kg and n_c is given by Fletcher's (1962) formula for the number concentration of ice nuclei (kg^{-1}),

$$n_c = 10^{-2}\exp[0.6(273.15 - T)]/\rho.$$

P_{II}, the initiation of ice crystals is given by

$$P_{II} = \max[(M_0 n_c - q_c)/\Delta t,\ 0], \tag{5.3.1.1.7}$$

as long as sufficient supersaturation over ice exists, where $M_0 = 10^{-12}$ kg.

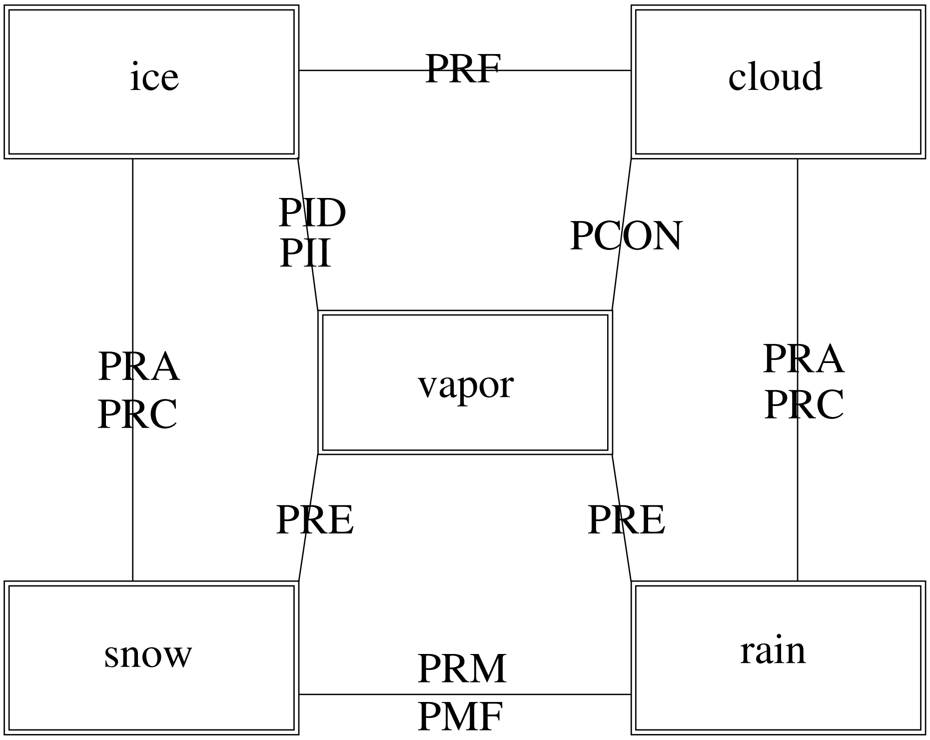

Figure 5.1 Box diagram illustrating the processes in the moisture scheme for ice (crystals), cloud(liquid), snow and rain. PCON, condensation/evaporation of cloud; PRA, accretion; PRC, conversion; PID, deposition onto ice crystals; PRE, evaporation for rain and deposition/sublimation for snow; PMF, melting/freezing due to advection; PII, initiation of ice crystals; and PRM, melting of snow due to fall.

P_{RA}, the accretion rate is given by

$$P_{RA} = \frac{1}{4}\pi \rho a q_c E N_0 \frac{\Gamma(3+b)}{\lambda^{3+b}}, \tag{5.3.1.1.8}$$

where Γ is the gamma-function, E is the collection efficiency (1 for rain and 0.1 for snow) and λ is given by

$$\lambda = \left(\frac{\pi N_0 \rho_w}{\rho q_r}\right)^{1/4}.$$

Here ρ_w is the mean density of rain or snow particles (1000 and 100 kg m^{-3}, respectively.)

P_{ID}, the deposition onto or sublimation of ice particles is found from

$$P_{ID} = \frac{4 D_i (S_i - 1)\rho n_c}{A + B}, \tag{5.3.1.1.9}$$

where

$$S_i = q_v / q_{si},$$

$$A = \frac{L_s^2 \rho}{K_a R_v T^2}, \quad B = \frac{1}{q_{si}\chi}.$$

L_s is the latent heat of sublimation, K_a is the thermal conductivity of air, R_v is the gas constant for water vapor, and χ is the diffusivity of vapor in air. The mean diameter of ice crystals, D_i, is found from the mean mass, $M_i = q_c/n_c$, and the mass-diameter relation for hexagonal plates from Rutledge and Hobbs (1983), $D_i = 16.3 M_i^{1/2}$ meters.

P_{RE}, the evaporation of rain and sublimation/deposition of snow can be determined from

$$P_{RE} = \frac{2\pi N_0 (S - 1)}{A + B}\left[\frac{f_1}{\lambda^2} + f_2 \left(\frac{a\rho}{\mu}\right)^{1/2} S_c^{1/3} \frac{\Gamma(5/2 + b/2)}{\lambda^{5/2+b/2}}\right], \tag{5.3.1.1.10}$$

with the relevant N_0, a, and b chosen for rain or snow, and $S = S_w$ or S_i. The definition of A and B also change from the above for rain, substituting L_v for L_s and q_{sw} for q_{si}. For snow, 2π is replaced by 4. The values of f_1 and f_2 are 0.78 and 0.32 for rain and 0.65 and 0.44 for snow. The term in brackets represents a distribution-integrated ventilation factor, $F = f_1 + f_2 S_c^{1/3} Re^{1/2}$, with $S_c = \mu/\rho\chi$, the Schmidt number, and $Re = V(D) D\rho/\mu$, the Reynolds number, and μ is the dynamic viscosity of air.

P_{CON}, the condensation is determined as follows. Temperature, water vapor mixing ratio and cloud water are forecast first: these preliminary forecast values are designated by T^*, q_v^* and q_c^*. We define

$$\delta M \ = \ q_v^* \ - \ q_{vs}^*,$$

where q_{vs}^* is the saturated mixing ratio at temperature T^*,

(1) if $\delta M \ > \ 0$ (supersaturation),

$$P_{CON} \ = \ \frac{r_1 \delta M}{\Delta t}, \tag{5.3.1.1.11a}$$

where

$$r_1 \ = \ \frac{1}{1 \ + \ \frac{L_v^2 q_{vs}^*}{R_v c_{pm} T^{*2}}},$$

(2) if $\delta M \ < \ 0$ and $q_c \ > \ 0$ (evaporation),

$$P_{CON} \ = \ -\min\left[-\frac{r_1 \delta M}{\Delta t}, \frac{q_c^*}{\Delta t}\right], \tag{5.3.1.1.11b}$$

(3) if $\delta M \ < \ 0$ and $q_c \ = \ 0$,

$$P_{CON} \ = \ 0. \tag{5.3.1.1.11c}$$

The P_{CON} term is computed diagnostically so no iteration is needed.

Additionally, as snow falls through the 0 °C level, it immediately melts to rain. This process is given by

$$P_{RM} \ = \ -\frac{\rho g V_f q_r}{\Delta p}. \tag{5.3.1.1.12}$$

Advection of ice or snow downwards or of rain or cloud upwards through this level also melts or freezes the particles, where

$$P_{MF} \ = \ -\frac{\omega(q_c \ + \ q_r)}{\Delta p}. \tag{5.3.1.1.13}$$

In both cases, the 0 °C isotherm is taken to be at a full model level boundary. Melting occurs at the level immediately below this boundary and freezing above it.

The latent heating is thus

$$\dot{Q} \ = \ L(P_{RE} \ + \ P_{ID} \ + \ P_{II} \ + \ P_{CON}) \ + \ L_m(P_{RM} \ + \ P_{MF}), \tag{5.3.1.1.14}$$

where $L = L_v$ for $T > 0\ ^\circ\mathrm{C}$ and $L = L_s$ for $T < 0\ ^\circ\mathrm{C}$, and $L_m = L_s - L_v$.

The fall speed is mass-weighted and so is determined from

$$V_f = a\frac{\Gamma(4+b)}{6}\lambda^{-b}. \qquad (5.3.1.1.15)$$

The fall term in (5.3.1.1.3), the rain and snow prediction equation, may be calculated on split time-steps, $\Delta t'$, in the explicit moisture routine. This ensures that $V_f \Delta t'/\Delta z < 1$, which is required for numerical stability. The size of $\Delta t'$ is determined independently in each model column based on the maximum value of $V_f \Delta t/\Delta z$ in the column, where Δt is the model time step.

5.3.1.2 Mixed-Phase Ice Scheme

This scheme is based on the simple ice phase scheme described in the previous subsection, but it does not immediately freeze or melt water and ice. Supercooled water can exist below 0°C in this scheme, as can unmelted snow exist above 0°C. Separate arrays are used to store vapor, cloud, rain, cloud ice and snow.

Homogeneous freezing of cloud water to cloud ice occurs immediately below -40°C and cloud ice melts immediately above 0°C. Snow melts according to

$$P_{SM} \;=\; -\,\frac{2\pi N_{0s}}{L_f} K_a(T - T_0) \left[\frac{f_1}{\lambda^2} \;+\; f_2 \left(\frac{a\rho}{\mu} \right)^{1/2} S_c^{1/3} \frac{\Gamma(5/2 \;+\; b/2)}{\lambda^{5/2+b/2}} \right], \qquad (5.3.1.2.1)$$

where $f_1 = 0.78$ and $f_2 = 0.31$ (Rutledge and Hobbs 1984), and the other constants are the ones relevant to snow in subsection (a). Evaporation of melting snow is modified to use the values of A and B for rain as in (5.3.1.1.10).

Heterogeneous freezing of cloud water to cloud ice is also included following Bigg (1953),

$$P_{CI} \;=\; B'\{\exp[A'(T_0 - T)] - 1\} \frac{\rho q_c^2}{\rho_w N_c} \qquad (5.3.1.2.2)$$

where $A' = 0.66\mathrm{K}^{-1}$, $B' = 100\mathrm{m}^{-3}\mathrm{s}^{-1}$ and the number concentration of cloud droplets per unit volume of air, $N_c = 10^{10}\mathrm{m}^{-3}$.

Sekhon and Srivastava (1970) determined that better comparison against observed snow distributions can be obtained in theoretical studies if the slope intercept value for the size distribution is expressed as

$$N_{0s}(m^{-4}) = 1.05 R^{-0.94} \qquad (5.3.1.2.3)$$

where, N_{0s} is the slope intercept and R (m s^{-1}) is the snow fall rate. Thus a variable intercept parameter replaces the constant N_{0s} used in the simple ice scheme.

This can be expressed in terms of snow mixing ratio, q_S, as

$$N_{0s} = \left\{ 1.05 \left[\frac{1}{\rho q_S \alpha} \left(\frac{\pi \rho_S}{\rho q_S} \right)^{\frac{b}{4}} \right]^{0.94} \right\}^{\frac{4}{0.94b+4}} \qquad (5.3.1.2.4)$$

where, $\alpha^{-1} = \frac{6\rho_w}{a\Gamma(4+b)}$.

5.3.2 Implicit cumulus parameterization schemes

5.3.2.1 The Kuo scheme

In this scheme, the amount of convection is determined by the vertically integrated moisture convergence. The feedback to the larger scale (the vertical distribution of heating and moistening), is determined with the help of the normalized vertical profiles of convective heating ($N_h(\sigma)$) and moistening ($N_m(\sigma)$), and a vertical eddy-flux divergence of water vapor associated with cumulus convection $V_{qf}(\sigma)$. Therefore, equations (2.1.3), (2.2.5) and (5.3.1.1.1) can be rewritten to include the convective-scale fluxes as

$$\frac{\partial p^*T}{\partial t} = -m^2\left[\frac{\partial p^*uT/m}{\partial x} + \frac{\partial p^*vT/m}{\partial y}\right] - \frac{\partial p^*T\dot{\sigma}}{\partial \sigma} + p^*\frac{\omega}{\rho c_p} + p^*\frac{L_v}{c_{pm}}N_h(\sigma)(1-b)gM_t + D_T, \quad (5.3.2.1.1)$$

$$\frac{\partial p^*T}{\partial t} = -m^2\left[\frac{\partial p^*uT/m}{\partial x} + \frac{\partial p^*vT/m}{\partial y}\right] - \frac{\partial p^*T\dot{\sigma}}{\partial \sigma} + T.DIV + \frac{1}{\rho c_p}\left[p^*\frac{Dp'}{Dt} - \rho_0 g p^* w - D_{p'}\right] + p^*\frac{L_v}{c_{pm}}N_h(\sigma)(1-b)gM_t + D_T, \quad (5.3.2.1.2)$$

$$\frac{\partial p^*q_v}{\partial t} = -m^2\left[\frac{\partial p^*uq_v/m}{\partial x} + \frac{\partial p^*vq_v/m}{\partial y}\right] + \delta_{nh}q_v DIV + p^*(-P_{RE} - P_{CON} - P_{II} - P_{ID}) + p^*\, bgM_tN_m(\sigma) + p^*V_{qf}(\sigma) + D_{qv}, \quad (5.3.2.1.3)$$

where the vertically integrated moisture convergence M_t is

$$M_t = \left(\frac{m^2}{g}\right)\int_0^1 \frac{\nabla p^*\dot{V}q_v}{m}d\sigma. \quad (5.3.2.1.4)$$

A portion $(1-b)$ of M_t is assumed to condense and precipitate, where the remaining fraction b is assumed to moisten the grid column. Following Anthes(1977), b is a function of the mean relative humidity $\overline{RH}$ of the column, where

$$b = 2(1-\overline{RH}) \quad (5.3.2.1.5)$$

for $\overline{RH} \geq 0.5$, and $b = 1$ otherwise.

The vertical profiles of heating and moistening

The normalized, nondimensional functions for the vertical profiles of heating and moistening and the divergence of the vertical eddy flux of water vapor are subject to the constraints

$$\int_0^1 N_h(\sigma)d\sigma = 1, \tag{5.3.2.1.6}$$

$$\int_0^1 N_m(\sigma)d\sigma = 1, \tag{5.3.2.1.7}$$

$$\int_0^1 V_{qf}(\sigma)d\sigma = 0. \tag{5.3.2.1.8}$$

Anthes *et al.* (1987) assume simple relationships for these functions, which are derived from budget studies. For the convective heating profile, N_h, they observe that the convective heating often has a parabolic shape with a maximum in the upper half of the cloud. Hence

$$N_h(\sigma) = a_1 x^2 + a_2 x + a_3, \tag{5.3.2.1.9}$$

where

$$x = ln\sigma \tag{5.3.2.1.10}$$

with the boundary conditions:

$$N_h(\sigma) = 0, \qquad at \;\; x_b = ln\sigma_b, \;\; and \; x_u = ln\sigma_u \tag{5.3.2.1.11}$$

at cloudbase (σ_b) and cloud top (σ_u), and

$$N_h'(\sigma) = \frac{\partial N_h(\sigma)}{\partial \sigma} = 0 \tag{5.3.2.1.12}$$

at $\bar{x}$, which is defined as

$$\bar{x} = \frac{x_u + x_b}{2}, \tag{5.3.2.1.13}$$

where subscripts u and b stand for the top and the base of the cloud. Using (5.3.2.1.6), a_1 can be shown to be

$$a_1 = \frac{2}{x_u^3 - x_b^3 + x_u^2 x_b - x_u x_b^2}. \tag{5.3.2.1.14}$$

The vertical moistening profile, $N_m(\sigma)$, is simply given following Anthes (1977) as

$$N_m(\sigma) = \frac{(1 - RH(\sigma))q_v s(\sigma)}{\int_{\sigma_{ktop}}^1 (1 - RH(\sigma'))q_{vs}(\sigma')d\sigma'}. \tag{5.3.2.1.15}$$

Divergence of the Vertical Eddy Flux of Water Vapor $V_{qf}(\sigma)$

The divergence of the vertical eddy flux of water vapor is defined as

$$V_{qf}(\sigma) = \frac{\partial \overline{\dot{\sigma}' q_v'}}{\partial \sigma}. \tag{5.3.2.1.16}$$

If one assumes a small fraction of convective cloud cover, and the cloud vertical motion $\dot{\sigma}_c$ is much larger than the larger-scale vertical motion, $\dot{\sigma}$ (5.3.2.1.16) can be rewritten as

$$V_{qf}(\sigma) = \frac{a}{1-a}\frac{\partial}{\partial \sigma}[\dot{\sigma}_c(q_{vc} - q_v)], \tag{5.3.2.1.17}$$

where q_{vc} is the mixing ratio in the cloud.

According to Anthes (1977), the fractional coverage a is calculate using

$$a = \frac{(1-b)gM_t}{\int_0^{p^*}\left(-\omega_c \frac{\partial q_{vc}}{\partial p} + \frac{\partial q_{vc}}{\partial t_e}\right)dp}, \tag{5.3.2.1.18}$$

which is the ratio between the grid-average condensation rate and that of a single cloud. The term $\frac{\partial q_{vc}}{\partial t_e}$ represents the contribution to the rate of change of cloud-mixing ratio by entrainment (Anthes 1977). Anthes *et al.* (1987) assume a typical value for the denominator of approximately $4.3 \times 10^{-3} cb\ s^{-1}$ and then rewrite (5.3.2.1.17) as

$$V_{qf}(\sigma) = \frac{(1-b)gM_t}{4.3 \times 10^{-3}}\frac{\partial}{\partial \sigma}[\dot{\sigma}_c(q_{vc} - q_v)]. \tag{5.3.2.1.19}$$

For further simplification, Anthes *et al.* (1987) next assume that $\dot{\sigma}_c$ also has a parabolic shape and can be expressed as

$$\dot{\sigma}_c = c_1 x^2 + c_2 x + c_3, \tag{5.3.2.1.20}$$

where $x = lnp$, and $\dot{\sigma}_c = 0$ at cloud-top and base. Furthermore, $q_{vc} - q_v$ is assumed to have a parabolic profile with pressure

$$q_{vc} - q_v = b_1 x^2 + b_2 x + b_3 \tag{5.3.2.1.21}$$

with

$$x = ln[(1-\sigma)(100 - p_t) + p_t]. \tag{5.3.2.1.22}$$

The procedure

The simple procedure can be summarized as follows:

1. Compute M_t from (5.3.2.1.4)
2. Check whether $M_t \geq 3. \times 10^{-5} kg\ m^{-2}\ s^{-1}$, a critical threshold value.
3. Check the model sounding for convective instability to see if convection is possible.
4. Determine cloud top and base from sounding.
5. Check whether cloud-depth is larger than a critical value ($\Delta\sigma \geq .3$)
6. Calculate the normalized vertical profile functions
7. Calculate $\dot{\sigma}_c$ on the full σ levels from (5.3.2.1.20)
8. Compute $q_{vc} - q_v$ from (5.3.2.1.21)
9. Calculate V_{qf} from (5.3.2.1.19)

5.3.2.2 A modified Arakawa-Schubert scheme

The version of the Arakawa-Schubert scheme used here was developed by Grell (1993). In contrast to the original scheme (Arakawa and Schubert 1974, AS), it includes moist convective-scale downdrafts. Other changes have been implemented to also allow the scheme to be used successfully in mesoscale models in mid-latitudes (Grell *et al.* 1991). To simplify the description we have adapted a terminology originally introduced by Betts (1974), which splits the parameterization problem from the modeling view in three parts: static control, dynamic control, and feedback. The static control includes usually a cloud-model and calculates cloud thermodynamic properties, the dynamic control is what determines the amount and location of the convection, and the feedback determines the vertical distribution of the integrated heating and moistening.

Static control

As with all commonly used one dimensional steady state cloud models (plumes, bubbles, or jets), our AS scheme makes use of the assumption that entrainment occurs over the depth of the buoyant element according to the entrainment hypothesis

$$\mu = \frac{1}{m(z)}\frac{\partial m(z)}{\partial z} \approx \frac{.2}{r}, \tag{5.3.2.2.1}$$

where μ is the total net fractional entrainment rate of the buoyant element, m its mass flux (m_u for updraft, m_d for downdraft), and r its radius. Following AS, the dependence on the radius is not explicitly used. However, implicitly, the radius of the cloud is assumed to be constant. Detrainment was originally only assumed to happen at the cloud top, but this assumption may easily be varied (Houze *et al.* 1979, Lord 1978) by defining a fractional detrainment rate, μ_{ud}, and rewriting (5.3.2.2.1) for the updraft of cloud type λ as

$$\begin{aligned} \mu_u = \mu_{ue} - \mu_{ud} &= \frac{1}{m_u(z)}\frac{\partial m_u(z)}{\partial z} \\ &= \frac{1}{m_u(\lambda,z)}\left(\left(\frac{\partial m_u(\lambda,z)}{\partial z}\right)_{ent} - \left(\frac{\partial m_u(\lambda,z)}{\partial z}\right)_{det}\right) \end{aligned} \tag{5.3.2.2.2}$$

where μ_{ue} is the gross fractional entrainment rate, and μ_u is the total net fractional entrainment rate of the updraft. Subscripts *ent* and *det* indicate changes due to entrainment and detrainment, respectively. Looking at the budget of a thermodynamic variable in an infinitesimal layer of the updraft we get

$$\frac{\partial m_u \alpha_u}{\partial z} = \left(\frac{\partial m_u}{\partial z}\right)_e \tilde{\alpha} - \left(\frac{\partial m_u}{\partial z}\right)_d \alpha_u + S_u. \tag{5.3.2.2.3}$$

Together with (5.3.2.2.2) this leads to the steady state plume equation

$$\frac{\partial \alpha_u(\lambda, z)}{\partial z} = \mu_{ue}(\tilde{\alpha}(z) - \alpha_u(\lambda, z)) + S_u \tag{5.3.2.2.4}$$

where α is a thermodynamic variable, the tilde denotes an environmental value, and subscript u denotes an updraft property. S stands for sources or sinks. Similarly, for the downdraft, we can rewrite equations (5.3.2.2.2) and (5.3.2.2.4) as

$$\begin{aligned} \mu_d = \mu_{de} - \mu_{dd} &= -\frac{1}{m_d(z)} \frac{\partial m_d(z)}{\partial z} \\ &= -\frac{1}{m_d(z)} \left(\left(\frac{\partial m_d(z)}{\partial z}\right)_{ent} - \left(\frac{\partial m_d(z)}{\partial z}\right)_{det} \right) \end{aligned} \tag{5.3.2.2.5}$$

and

$$\frac{\partial \alpha_d(z)}{\partial z} = -\mu_{de}(\tilde{\alpha}(z) - \alpha_d(z)) + S, \tag{5.3.2.2.6}$$

where subscript d denotes a downdraft property. For moist static energy

$$\tilde{h}(z) = C_p \tilde{T}(z) + gz + L\tilde{q}(z), \tag{5.3.2.2.7}$$

equations (5.3.2.2.4) and (5.3.2.2.6) simply become

$$\frac{\partial h_u(\lambda, z)}{\partial z} = \mu_{ue}(\tilde{h}(z) - h_u(\lambda, z)) \tag{5.3.2.2.8}$$

and

$$\frac{\partial h_d(z)}{\partial z} = -\mu_{de}[\tilde{h}(z) - h_d(z)]. \tag{5.3.2.2.9}$$

Next, for the moisture budget of the updraft, we use

$$\alpha_u = q_u(\lambda, z) + q_l(\lambda, z) \tag{5.3.2.2.10}$$

and

$$S_u = -c_0 m_u(\lambda, z) q_l(\lambda, z). \tag{5.3.2.2.11}$$

Here S_u is the total water that is rained out, c_0 is a rainfall conversion parameter and could be a function of cloud size or wind shear, q_l is the suspended liquid water content of the cloud, and q_u is the water vapor mixing ratio inside the updraft. Equation (5.3.2.2.4) can then be rewritten as

$$\frac{\partial(q_u(\lambda,z)+q_l(\lambda,z))}{\partial z}=\mu_{ue}(\tilde{q}(z)-q_u(\lambda,z)-q_l(\lambda,z))+S_u. \tag{5.3.2.2.12}$$

For the downdraft, the equation for the water vapor reads

$$\frac{\partial q_d(z)}{\partial z}=-\mu_{de}[\tilde{q}(z)-q_d(z)]+S_d. \tag{5.3.2.2.13}$$

S_d here is a source; namely the evaporation of rain. Assuming saturation in the updraft and downdraft, we can make use of the approximate equation

$$q_c(\lambda,z)=\tilde{q}^*+\frac{\gamma}{1+\gamma}\frac{1}{L}[h_c(\lambda,z)-\tilde{h}^*(z)], \tag{5.3.2.2.14}$$

where

$$\gamma=\frac{L}{c_p}\left(\frac{\partial\tilde{q}^*}{\partial T}\right)_P \tag{5.3.2.2.15}$$

the asterisk denotes a saturated value, and h_c here stands for the moist static energy in the cloud (updraft or downdraft), if saturation is assumed. Next, to arrive at a usable closure, the up- and down-draft mass fluxes are normalized by the updraft base ($m_b(\lambda)$) mass flux, and the downdraft base $m_0(\lambda)$ mass flux of a subensemble. Hence, for the updraft,

$$m_u(\lambda,z)=m_b(\lambda)\eta_u(\lambda,z) \tag{5.3.2.2.16}$$

and

$$\mu_{ue}-\mu_{ud}=\frac{1}{\eta_u(z)}\frac{\partial\eta_u(z)}{\partial z}. \tag{5.3.2.2.17}$$

Equivalently, for the downdraft we may write

$$m_d(z)=m_0(\lambda)\eta_d(\lambda,z) \tag{5.3.2.2.18}$$

and

$$\mu_{de}-\mu_{dd}=\frac{1}{\eta_d(z)}\frac{\partial\eta_d(z)}{\partial z}. \tag{5.3.2.2.19}$$

Here, m_0 is the mass flux at the originating level and η_d, as η_u in equation (5.3.2.2.16), is the normalized mass flux profile.

To leave only one unknown variable, we follow Houze *et al.* (1979) and make the originating mass flux of the downdraft a function of the updraft mass flux and reevaporation of convective condensate. Therefore, the condensate in the updraft

$$C_u(\lambda)d\lambda = m_b d\lambda \left(\int_{z_B}^{z_T} \eta_u(\lambda, z) S_u dz \right) \equiv I_1 m_b d\lambda \tag{5.3.2.2.20}$$

is apportioned according to

$$C_u(\lambda)d\lambda = (R_c(\lambda) + E_d(\lambda))d\lambda = (\alpha(\lambda) + \beta(\lambda))C_u(\lambda)d\lambda, \tag{5.3.2.2.21}$$

where $\alpha + \beta = 1$ and E_d, the evaporation of condensate in the downdraft for cloud type λ, can be written as

$$E_d d\lambda = m_0(\lambda)d\lambda \left(\int_0^{z_0} \eta_d(\lambda, z) S_d dz \right) \equiv I_2 m_0 d\lambda. \tag{5.3.2.2.22}$$

From equations (5.3.2.2.20-5.3.2.2.22) we see that

$$E_d d\lambda = \beta C_u d\lambda = \beta I_1 m_b d\lambda = I_2 m_0 d\lambda \tag{5.3.2.2.23}$$

and hence

$$m_0(\lambda) = \frac{\beta(\lambda) I_1 m_b(\lambda)}{I_2(\lambda)} = \epsilon(\lambda) m_b(\lambda). \tag{5.3.2.2.24}$$

Here $1-\beta$ is the precipitation efficiency. Following Fritsch and Chappell (1980), it is made dependent on the windshear.

To solve the above equations we need to specify boundary conditions as well as make some arbitrary assumptions. For the updraft we assume

$$h_u(z_b) = MAX(\tilde{h}(z)) \tag{5.3.2.2.25}$$

with

$$z \leq z_b$$

and

$$h_u(\lambda, z_T) = \tilde{h}^*(z_T), \tag{5.3.2.2.26}$$

where the asterisk denotes a saturation value. Similarly, for the downdraft,

$$h_d(z_0) = MIN(\tilde{h}(z)). \tag{5.3.2.2.27}$$

Physically, for both updraft and downdraft, we allow for maximum buoyancy. The boundary conditions for the updraft are different than in the original scheme, which had a rigid dependence on the planetary boundary layer height. In the original scheme, the mixed layer was assumed to be well mixed, and the cloud base was located on top of the mixed layer. In semi-prognostic tests (Grell *et al.* 1991) large variations of moist static energy profiles were found in very low levels of the troposphere. This was caused by cold downdraft outflow. Naturally, the inflow to an updraft will not be a mixture of downdraft air and the more buoyant air; it is more likely the air with high moist static energy from the layer above the downdraft outflow. Furthermore, compensatory subsidence should only continue to the level from which the updraft draws its air. Compensatory uplifting may be required in very low layers of the troposphere because of the downdraft mass flux.

Feedback

The feedback to the larger-scale environment is expressed in a convenient form as

$$\left(\frac{\partial s}{\partial t}\right)_{cu} = \frac{1.}{\rho}\frac{\partial}{\partial z}F_{s-Ll}, \tag{5.3.2.2.28}$$

$$\left(\frac{\partial q}{\partial t}\right)_{cu} = -\frac{1.}{\rho}\frac{\partial}{\partial z}F_{q+l} - R, \tag{5.3.2.2.29}$$

where s is the dry static energy ($s = c_pT + gz$). The convective-scale fluxes within a grid box are defined as

$$F_{s-Ll} \equiv F_s - LF_l \tag{5.3.2.2.30}$$

$$F_{q+l} \equiv F_q + F_l \tag{5.3.2.2.31}$$

where F_s is the flux of dry static energy, F_q is the flux of water vapor, and F_l is the flux of suspended cloud liquid water. These are defined as

$$\begin{aligned} F_s(z) \equiv &+ \int_\lambda \eta_u(\lambda, z)[s_u(\lambda, z) - \bar{s}(z)]m_b(\lambda)d\lambda \\ &- \int_\lambda \eta_d(\lambda, z)[s_d(\lambda, z) - \bar{s}(z)]m_0(\lambda)d\lambda \end{aligned} \tag{5.3.2.2.32}$$

$$F_q(z) \equiv + \int_\lambda \eta_u(\lambda, z)[q_u(\lambda, z) - \bar{q}(z)]m_b(\lambda)d\lambda - \int_\lambda \eta_d(\lambda, z)[q_d(\lambda, z) - \bar{q}(z)]m_0(\lambda)d\lambda \tag{5.3.2.2.33}$$

$$F_l(z) \equiv \int_\lambda \eta_u(\lambda, z)l(\lambda, z)m_b(\lambda)d\lambda \tag{5.3.2.2.34}$$

The rainfall (convective-scale sink of cloud water) is defined as

$$R(z) \equiv + \int_\lambda \eta_u(\lambda, z)c_0(\lambda)l(\lambda, z)m_b(\lambda)d\lambda - \int_\lambda \eta_d(\lambda, z)q_e(\lambda, z)m_0(\lambda)d\lambda \tag{5.3.2.2.35}$$

Here q_e is the amount of moisture that is necessary to keep the downdraft saturated. The second term on the righthand sides is due to downdrafts and is zero above the downdraft-originating level. Below the updraft-air originating level, the first term on the right-hand sides is zero and only downdrafts affect the larger-scale environment. Below the updraft-air originating level, the convective-scale fluxes due to updrafts are zero. Between the updraft-air-originating level and the level of free convection (the LFC), F_l and R are set to zero. Since no liquid water is assumed to be in the environment as the downdraft, the downward flux due to updrafts as well as downdraft fluxes in equation (5.3.2.2.33) are zero. Schubert (1974) showed that convection will not increase the total moist static energy per unit area in a column. In essence, only precipitation can change the dry static energy budget and the total mass of water vapor. All variables in the flux terms can be determined from the equations for the static control, except $m_b(\lambda)$. This is determined in the dynamic control, which incorporates the closure assumption of the scheme and is described next.

Dynamic control

Arakawa-Schubert first introduced the cloud work function, which is an integral measure of the buoyancy force associated with a subensemble. Starting with

$$\frac{dw_u}{dt} = B_u - F_r = \frac{dw_u}{dz}\frac{dz}{dt} = \frac{d}{dt}\frac{d}{dz}\frac{w_u^2}{2} = \frac{1}{w_u}\frac{d}{dt}\frac{w_u^2}{2}, \tag{5.3.2.2.36}$$

where B_u is the acceleration due to buoyancy and F_r the deceleration due to friction, and multiplying equation (5.3.2.2.36) by $\rho_u(\lambda, z)w_u(\lambda, z)$, gives

$$\frac{d}{dt}\rho_u\frac{w_u^2}{2} = \rho_u w_u(B_u - F_r). \tag{5.3.2.2.37}$$

Integrating over the depth of the updraft and using $m_u = \rho_u w_u = m_b\eta_u$ yields

$$\frac{d}{dt}\int_{z_b}^{z_T}\rho_u\frac{w_u^2}{2}dz = m_b(\lambda)\int_{z_b}^{z_T}\eta_u B_u dz - D_u, \tag{5.3.2.2.38}$$

where D is the updraft-scale kinetic energy dissipation. Equation (5.3.2.2.38) can be written in the symbolic form

$$\frac{d}{dt}\overline{KE}_u = A_u(\lambda)m_b(\lambda) - D_u(\lambda), \tag{5.3.2.2.39}$$

where $A_u(\lambda)$ is a measure of the efficiency of kinetic energy generation inside the cloud and is called the cloud work function. It can also be written as

$$A_u(\lambda) = \int_{z_B}^{z_T}\frac{g}{C_pT(z)}\frac{\eta_u(\lambda, z)}{1+\gamma}(h_u(\lambda, z) - \tilde{h}^*(z))dz, \tag{5.3.2.2.40}$$

where γ is defined as in equation (5.3.2.2.15). As with equations (5.3.2.2.36-5.3.2.2.38), defining a kinetic energy generation inside the downdraft leads to

$$\frac{d}{dt}\overline{KE_d} = A_d(\lambda)m_0(\lambda) - D_d(\lambda), \tag{5.3.2.2.41}$$

where A_d, the measure of the efficiency of kinetic energy generation inside the downdraft, can be written as

$$A_d(\lambda) = \int_{z_0}^{z_{sur}}\frac{g}{C_pT(z)}\frac{\eta_d(\lambda, z)}{1+\gamma}(\tilde{h}^*(z) - h_d(\lambda, z))dz. \tag{5.3.2.2.42}$$

Note that dry static energy instead of moist static energy would have to be used if subsaturation is assumed. We can combine equation (5.3.2.2.39) and (5.3.2.2.41) and then make use of (5.3.2.2.24) to yield

$$\frac{d}{dt}\overline{KE_{tot}} = A_{tot}(\lambda)m_b(\lambda) - D_{tot}(\lambda), \tag{5.3.2.2.43}$$

where

$$A_{tot}(\lambda) = A_u(\lambda) + \epsilon(\lambda) A_d(\lambda) \tag{5.3.2.2.44}$$

is the total cloud work function which was redefined as a measure of the efficiency of kinetic energy generation in updrafts as well as downdrafts. Next, AS separated the change of the cloud work function into two parts: One is due to the change in the larger-scale variables

$$\left(\frac{dA_{tot}}{dt}\right)_{LS} \equiv F(\lambda), \tag{5.3.2.2.45}$$

and one is due to the modification of the environment by the clouds. Since the cumulus feedback on the larger-scale fields is a linear function of m_b, this term can be written in the symbolic form

$$\left(\frac{dA_{tot}}{dt}\right)_{CU} \equiv \int\limits_{\lambda} K(\lambda, \lambda') m_b(\lambda') d\lambda. \tag{5.3.2.2.46}$$

Therefore

$$\frac{dA_{tot}}{dt} = F(\lambda) + \int\limits_{\lambda} K(\lambda, \lambda') m_b(\lambda') d\lambda, \tag{5.3.2.2.47}$$

where $K(\lambda, \lambda')$ are the kernels. The kernels are an expression for the interaction between clouds (updrafts and downdrafts). Equation (5.3.2.2.47) is solved with a linear programming method (Lord 1978).

In the original version of the Arakawa-Schubert scheme, the fractional entrainment rate was the parameter which characterized the cloud. In later papers, the cloud-top detrainment level was chosen instead. If a fine vertical resolution is assumed, the second choice will most likely be better numerically, since no interpolation is necessary at the cloud tops. However, in the extremely unstable environment of the mid-latitudes, it is sometimes impossible to calculate "clouds" with cloud tops in the unstable layers. Entrainment rates would have to be extremely large to stop cloud growth. We therefore chose the fractional entrainment rate as the spectral parameter.

The procedure

The cloud base is a function of time and space. However, at a specific grid point the cloud base will be the same for every member of the subensemble. We also distinguish among an updraft-air originating level, z_u, a downdraft-air originating level, z_0, a cloud base level, z_b (the LCL), and a level of free convection, z_{bc} (LFC). Here, z_u is determined from condition (5.3.2.2.25) and determines the thermodynamic properties of the updraft from cloud type i. The air becomes saturated at z_b; condensation will start, but no convection can occur yet because the buoyancy is negative. In some instances this level could be the same as the LFC. The LFC is of great importance since this is the level at which the static control starts the calculations of individual convective elements. Since the air that feeds the cloud originates below the LCL, compensatory subsidence is allowed to reach the originating level of the updraft air.

For the downdraft, the originating level is also a function of time and space. If the downdraft exists, it will always reach the surface.

For updraft and downdraft in layer k the mass budgets are defined as

$$e_u(k,i) - d_u(k,i) = \eta_u(k+.5,i) - \eta_u(k-.5,i) \qquad (5.3.2.2.48a)$$

and

$$e_d(k,i) - d_d(k,i) = \eta_d(k+.5,i) - \eta_d(k-.5,i), \qquad (5.3.2.2.48b)$$

where entrainment for the updraft and downdraft is defined as

$$e_u(k,i) = \mu_{ue}\Delta z_d \, \eta_u(k+.5,i) \qquad (5.3.2.2.49a)$$

$$e_d(k,i) = \mu_{de}\Delta z_d \, \eta_d(k-.5,i) \qquad (5.3.2.2.49b)$$

and detrainment is defined as

$$d_u(k,i) = \mu_{ud}\Delta z_d \, \eta_u(k+.5,i) \qquad (5.3.2.2.50a)$$

$$d_d(k,i) = \mu_{dd}\Delta z_d \, \eta_d(k-.5,i). \qquad (5.3.2.2.50b)$$

Combining the above three equations for the updraft and downdraft yields

$$\eta_u(k-.5,i) = \eta_u(k+.5,i)(1. + \mu_{ue}\Delta z_d - \mu_{ud}\Delta z_d) \qquad (5.3.2.2.51a)$$

for the updraft and

$$\eta_d(k+.5,i) = \eta_d(k-.5,i)(1. + \mu_{de}\Delta z_d - \mu_{dd}\Delta z_d) \qquad (5.3.2.2.51b)$$

for the downdraft. Here we define $\Delta z_d = z(k+.5) - z(k-.5)$. The discretized form for the downdraft moist static energy budget reads

$$\begin{aligned} & e_d(k,i)\tilde{h}(k) - d_d(k,i)\frac{h_d(k+.5,i) - h_d(k-.5,i)}{2} \\ & = \eta_d(k+.5,i)h_d(k+.5,i) - \eta_d(k-.5,i)h_d(k-.5,i) \end{aligned}. \tag{5.3.2.2.52}$$

Using equations (5.3.2.2.48)-(5.3.2.2.51) in equation (5.3.2.2.52) leads to

$$h_d(k+.5,i) = \frac{h_d(k-.5,i)(1. - .5\mu_{dd}\Delta z_d) + \mu_{de}\Delta z_d\,\tilde{h}(k)}{1. + \mu_{de}\Delta z_d - \mu_{dd}\Delta z_d + .5\mu_{dd}\Delta z_d}. \tag{5.3.2.2.53}$$

The moisture budget for the downdraft is developed in several steps. First, the downdraft water vapor mixing ratio before evaporation, but after entrainment, is calculated. This is done using

$$q_d(k,i) = \frac{q_d(k-.5,i)(1. - .5\mu_{dd}\Delta z_d) + \mu_{de}\Delta z_d\,\tilde{q}(k)}{1. + \mu_{de}\Delta z_d - \mu_{dd}\Delta z_d + .5\mu_{dd}\Delta z_d}. \tag{5.3.2.2.54}$$

Next, equations (5.3.2.2.14) and (5.3.2.2.15) give the mixing ratio, q_{vd}, that the updraft or downdraft would have if saturated. Hence, the amount of moisture that is necessary to keep the downdraft from cloud type i saturated in layer k is

$$q_e(k,i) = -[q_d(k,i) - q_{vd}(k,i)]. \tag{5.3.2.2.55}$$

Next we check whether the updraft produces enough rain to sustain saturation in the downdraft by requiring that

$$\sum c_0\Delta z(k)\,\eta_u(k-.5,i)q_l(k-.5,i) - \sum \epsilon(i)\Delta z(k)\,\eta_d(k+.5,i)q_e(k,i) > 0. \tag{5.3.2.2.56}$$

If this is not the case, a downdraft is not allowed to exist.

Having defined the discretized versions of the equations from the static control, we now can describe the procedure.

Using the larger-scale temperature and moisture fields (T_0, q_0) at time t_0, and given a functional or empirical relationship for μ_d, μ_{de}, and μ_{dd}, the equations from the static control are used to calculate $\mu_{ue}, h_u(z,i), h_d(z,i), q_u(z,i), q_d(z,i), \eta_u(z,i)$, and $\eta_d(z,i)$ for cloud type i. These are needed to determine the total cloud work function A_{tot} using

$$A_{tot}(i) = A_u(i) + \epsilon A_d(i). \tag{5.3.2.2.57}$$

The discretized versions of equations (5.3.2.2.40) and (5.3.2.2.42) that are used to determine the cloud work functions for updrafts and downdrafts are

$$
\begin{aligned}
A_u(i) = \sum_{k=LFC}^{k=ktop} \Bigg[& \frac{g}{c_p\, T(k-.5)} \eta_u(k-.5,i) \\
& * \left(\frac{h_u(k-.5,i) - \tilde{h}^*(k-.5)}{1+\gamma(k-.5)} \right) \\
& * (z(k-1) - z(k)) \Bigg]
\end{aligned}
\tag{5.3.2.2.58}
$$

and

$$
\begin{aligned}
A_d(i) = \sum_{k=z_0}^{k=sur} \Bigg[& \frac{g}{c_p\, T(k-.5)} \eta_d(k-.5,i) \\
& * \left(\frac{h_d(k-.5,i) - \tilde{h}^*(k-.5)}{1+\gamma(k-.5)} \right) . \\
& * (z(k) - z(k-1)) \Bigg]
\end{aligned}
\tag{5.3.2.2.59}
$$

The kernels of cloud type i are by definition the changes of the cloud work functions due to another subensemble, i'. Thus, following Lord (1978), T_0 and q_0 are modified by an arbitrary amount of mass flux, $m_b' \Delta t'$, from the i' subensemble. This is done for every possible subensemble and can be written in the symbolic form

$$
\bar{T}'(k,i) = \bar{T}(k) + \delta_{i'}(\bar{T}(k)) m_b' \Delta t', \tag{5.3.2.2.60}
$$

$$
\bar{q}'(k,i) = \bar{q}(k) + \delta_{i'}(\bar{q}(k)) m_b' \Delta t'. \tag{5.3.2.2.61}
$$

The δ terms, which are changes per unit $m_b(i)$, are easily calculated from budget considerations as in Lord (1978). With the downdraft terms, the moist static energy budget of layer k and cloud type i becomes

$$
\begin{aligned}
\frac{\Delta p(k)}{g} \delta_{i'}(\tilde{h}(k,i)) = & + (\eta_u(k-.5,i) - \epsilon(i)\eta_d(k-.5,i))\tilde{h}(k-.5) \\
& - (\eta_u(k+.5,i) - \epsilon(i)\eta_d(k+.5,i))\tilde{h}(k+.5) \\
& - (e_u(k,i) + \epsilon(i) e_d(k,i))\tilde{h}(k) \qquad , \\
& + d_u(k,i) \frac{h_u(k+.5,i) + h_u(k-.5,i)}{2} \\
& + \epsilon(i) d_d(k,i) \frac{h_d(k+.5,i) + h_d(k-.5,i)}{2}
\end{aligned}
\tag{5.3.2.2.62}
$$

where $e_u(k,i) and d_u(k,i)$ are the entrainment and detrainment for the updraft, and $\Delta p(k)$ is defined by $\Delta p(k) = p(k+.5) - p(k-.5)$. A simple physical interpretation of the terms on the righthand side can be understood by looking at Fig. 5.2. The first term is the subsidence on top of the layer, the second is the subsidence on the bottom of the layer. This subsidence is an environmental compensatory mass flux due to the updraft and downdraft mass fluxes inside the cloud. Note that below z_u the "compensatory subsidence" may be compensatory uplifting, since in that case only downdrafts exist. The third term represents entrainment into the updraft and downdraft; the fourth term represents detrainment from the edges of the updraft; the fifth term represents detrainment from the edges of the downdraft.

For the moisture budget,

$$\begin{aligned}\frac{\Delta p(k)}{g}\delta_{i'}(\tilde{q}(k,i)) = &+(\eta_u(k-.5,i)-\epsilon(i)\eta_d(k-.5,i))\tilde{q}(k-.5)\\ &-(\eta_u(k+.5,i)-\epsilon(i)\eta_d(k+.5,i))\tilde{q}(k+.5)\\ &-(e_u(k,i)+\epsilon(i)e_d(k,i))\tilde{q}(k)\\ &+d_u(k,i)\frac{q_u(k+.5,i)+q_u(k-.5,i)}{2}\\ &+\epsilon(i)d_d(k,i)\frac{q_d(k+.5,i)+q_d(k-.5,i)}{2}\end{aligned} \quad . \tag{5.3.2.2.63}$$

At the cloud top, downdrafts have no effects and updrafts detrain all their mass.

$$\begin{aligned}\frac{\Delta p(ktop)}{g}\delta_{i'}(\tilde{h}(ktop,i)) = &-\eta_u(ktop+.5,i)\tilde{h}(ktop+.5)\\ &-e_u(ktop,i)\tilde{h}(ktop)\\ &+d_u(ktop,i)\frac{h_u(ktop+.5,i)+h_u(ktop,i)}{2}+\eta_u(ktop,i)h_u(ktop,i)\end{aligned} \tag{5.3.2.2.64}$$

and

$$\begin{aligned}\frac{\Delta p(ktop)}{g}\delta_{i'}(\tilde{q}(ktop,i)) = &-\eta_u(ktop+.5,i)\tilde{q}(ktop+.5)\\ &-e_u(ktop,i)\tilde{q}(ktop)\\ &+d_u(ktop,i)\frac{q_u(ktop+.5,i)+q_u(ktop,i)}{2}+\eta_u(ktop,i)q_u(ktop,i)\end{aligned} \quad . \tag{5.3.2.2.65}$$

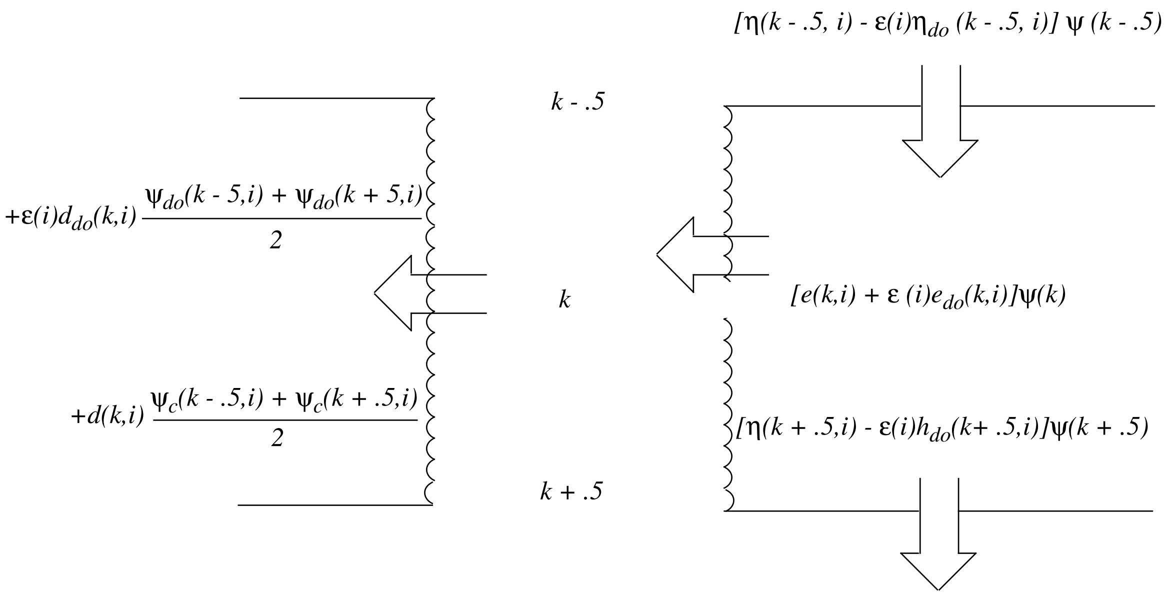

Figure 5.2 Illustration of budget for thermodynamic variable ψ in layer *k*.

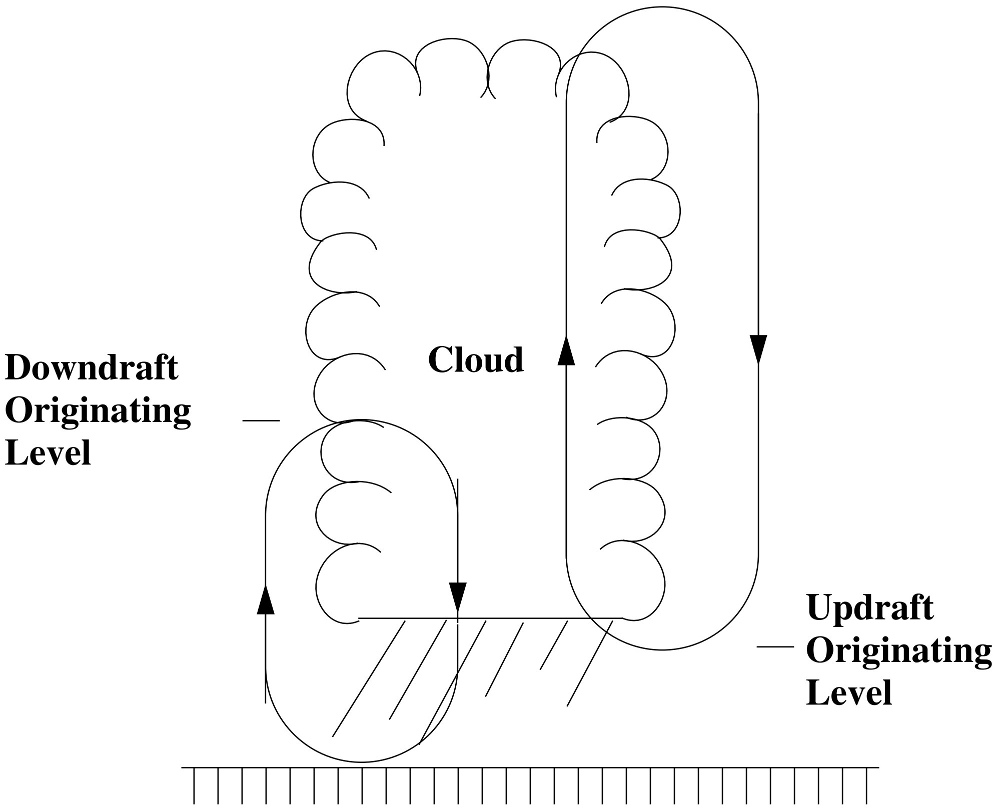

Figure 5.3 Conceptual picture of convection parameterized in Grell scheme.

Here $\Delta p(ktop) = p(ktop+.5) - p(ktop-.5)$. Note that in the fourth term we have included the detrainment of all the cloud mass at the cloud top. Finally, at the surface

$$\begin{aligned}\frac{\Delta p(ksur)}{g}\delta_{i'}(\tilde{h}(ksur,i)) =& -\epsilon(i)\eta_d(ksur-.5,i))\tilde{h}(ksur-.5)\\ &+\epsilon(i)\eta_d(ksur,i)h_d(ksur,i)\\ &-\epsilon(i)e_d(ksur-.5,i)\tilde{h}(ksur-.5)\\ &+\epsilon(i)d_d(ksur,i)\frac{h_d(ksur,i)+h_d(ksur-.5,i)}{2}\end{aligned} \tag{5.3.2.2.66}$$

and

$$\begin{aligned}\frac{\Delta p(ksur)}{g}\delta_{i'}(\tilde{q}(ksur,i)) =& -\epsilon(i)\eta_d(ksur-.5,i))\tilde{q}(ksur-.5)\\ &+\epsilon(i)\eta_d(ksur,i)q_d(ksur,i)\\ &-\epsilon(i)e_d(ksur-.5,i)\tilde{q}(ksur-.5)\\ &+\epsilon(i)d_d(ksur,i)\frac{q_d(ksur,i)+q_d(ksur-.5,i)}{2}\end{aligned}, \tag{5.3.2.2.67}$$

with $\Delta p(ksur) = p(ksur+.5) - p(ksur-.5)$. Here, the first term is the compensatory environmental mass flux, the second term is the detrainment of all downdraft air at the bottom, the third term is entrainment into the downdraft, and the fourth term is the detrainment of air around the downdraft edges.

The new thermodynamic fields, ${T_0}'(k,i')$ and ${q_0}'(k,i')$, are then used again from the static control to calculate new cloud properties and a new cloud work function, $A'_{tot}(i',i)$. Note that T'_0 and q'_0 are now functions of the subensemble i'. From the definition of the kernel we then can calculate the kernels simply as

$$K(i,i') = \frac{A'_{tot}(i',i) - A_{tot}(i)}{m_b``\Delta t``}. \tag{5.3.2.2.68}$$

Next, we go back to the original fields and modify those with the large-scale advective changes to get

$$T``(k) = T_0 + \left(\frac{\partial T}{\partial t}\right)_{ADV}\Delta t \tag{5.3.2.2.69}$$

and

$$q``(k) = q_0 + \left(\frac{\partial q}{\partial t}\right)_{ADV}\Delta t, \tag{5.3.2.2.70}$$

where (5.3.2.2.69) and (5.3.2.2.70) are applied over Δt= 30 min. The double prime quantities are then used again by the static control, which will calculate new cloud properties, and so new cloud work functions, $A_{tot}''(i)$, will be determined. Next, the large-scale forcing (by definition the change of the cloud work function due to large-scale effects only) is calculated using

$$F(i) = \frac{A_{tot}''(i) - A_{tot}(i)}{\Delta t}. \tag{5.3.2.2.71}$$

The large-scale forcing and the kernels are then both used by the dynamic control to estimate the cloud base mass flux distribution function, m_b, using an IMSL subroutine to solve the linear programming problem. Finally, the feedback to the larger-scale environment is simply given by

$$\left(\frac{\partial T(k)}{\partial t}\right)_{CU} = \sum_{i'=1}^{i'_{MAX}} \delta_i'(T(k))m_b(i') \tag{5.3.2.2.72}$$

and

$$\left(\frac{\partial q(k)}{\partial t}\right)_{CU} = \sum_{i'=1}^{i'_{MAX}} \delta_i'(q(k))m_b(i'), \tag{5.3.2.2.73}$$

where the precipitation can be calculated using

$$\begin{aligned} P = &\sum_{i'=1}^{i'_{MAX}} \sum_{k=1}^{k=ktop} c_0 \Delta z(k) q_l(k+.5,i) m_u(k+.5,i) \\ &- \sum_{i'=1}^{i'_{MAX}} \sum_{k=1}^{k=ktop} \Delta z(k) q_{ev}(k+.5,i) m_d(k+.5,i) \end{aligned}. \tag{5.3.2.2.74}$$

5.3.2.3 The Grell scheme

This is a very simple scheme that was constructed to avoid first-order sources of errors (Grell 1993). The very simplistic conceptual picture of how this parameterization is envisioned to function is shown in Fig. 5.3. Clouds are pictured as two steady-state circulations, caused by an updraft and a downdraft. There is no direct mixing between cloudy air and environmental air, except at the top and the bottom of the circulations. The cloud model that is used to calculate cloud properties in this scheme is formulated with only a few equations. Mass flux is constant with height, and there is no entrainment or detrainment along the cloud edges. We can simply write

$$m_u(z) = m_u(z_b) = m_b \tag{5.3.2.3.1}$$

and

$$m_d(z) = m_d(z_0) = m_0 \tag{5.3.2.3.2}$$

for the mass flux of the updraft (m_u) and the downdraft (m_d). Here m_b and m_0 are simply the mass fluxes of the updraft and downdraft at their originating level. If it is assumed that the conditions at originating levels are given by the environment, for any thermodynamic variable , the budget inside the cloud simply becomes

$$\alpha_u(z) = \tilde{\alpha}(z_b) + S_u(z) \ , \tag{5.3.2.3.3}$$

and

$$\alpha_d(z) = \tilde{\alpha}(z_0) + S_d(z), \tag{5.3.2.3.4}$$

where α is a thermodynamic variable, the tilde denotes an environmental value, and S stands for sources or sinks. For moist static energy

$$\tilde{h}(z) = C_p\tilde{T}(z) + gz + L\tilde{q}(z), \tag{5.3.2.3.5}$$

equations (3) and (4) simply become

$$h_u(z) = \tilde{h}(z_b) \tag{5.3.2.3.6}$$

and

$$h_d(z) = \tilde{h}(z_0). \tag{5.3.2.3.7}$$

For the moisture budget of the updraft we can make use of the approximate equations (5.3.2.2.14) and (5.3.2.2.15) to calculate the mixing ratio inside the cloud if saturation is assumed. Together with equations (5.3.2.3.3) and (5.3.2.3.4), this will give us S_u and S_d, the condensation and evaporation. Note also that no cloud water is assumed to exist; all water is converted to rain.

Given boundary conditions, equations (5.3.2.3.1)-(5.3.2.3.7) have two unknowns, m_b, and m_0. In order to leave only one unknown variable, the originating mass flux of the downdraft is made a function of the updraft mass flux and the reevaporation of convective condensate, as in the previous section (see equations (5.3.2.2.20)-(5.3.2.2.24)). Therefore,

$$m_0 = \frac{\beta I_1 m_b}{I_2} = \epsilon m_b. \tag{5.3.2.3.8}$$

Here, $1 - \beta$ is the precipitation efficiency. To specify boundary conditions, we assume

$$h_u(z) = h_u(z_b) = MAX(\tilde{h}(z)), \tag{5.3.2.3.9}$$

$$with \quad z \leq z_b, and$$

$$h_u(z_T) = \tilde{h}^*(z_T), \tag{5.3.2.3.10}$$

where the asterisk denotes a saturation value. Similarly, for the downdraft,

$$h_d(z) = h_d(z_0) = MIN(\tilde{h}(z)). \tag{5.3.2.3.11}$$

Physically, for both, updraft and downdraft, we allow for maximum buoyancy. For this deep convection scheme, the cloud base for the updraft is not restricted to the boundary layer, but can be anywhere in the troposphere.

Feedback to the larger-scale equations

To avoid zero-order sources of errors, the feedback must include the cooling effects of moist convective downdrafts. Furthermore, lateral mixing should never be excessive, especially if the cloud properties have been calculated with a steady-state cloud model. Keeping in mind the conceptual picture in Fig. 5.3, the feedback for this scheme is entirely determined by compensating mass fluxes and detrainment at cloud top and bottom. Conceptually, no averaging (such as the normally used top-hat or Reynolds averaging methods) is necessary. This does not mean that scale-separation is not required, but for this parameterization it is not necessary to assume that the fractional area coverage is very small. Note, however, that any parameterization can only make sense if a clear scale separation exists. None of the parameterized effects may be resolved by the larger-scale.

Assuming that the conceptual picture in Fig. 5.3 happens in only one grid box, we can express the changes caused by the convection as

$$\left(\frac{\partial \tilde{h}(k)}{\partial t}\right)_{CU} = \frac{\partial h_u(z) m_b}{\partial z} - \frac{\partial \tilde{h}(z) m_b}{\partial z} - \frac{\partial h_d(z) m_0}{\partial z} + \frac{\partial \tilde{h}(z) m_0}{\partial z} \qquad (5.3.2.3.12)$$

and

$$\left(\frac{\partial q(k)}{\partial t}\right)_{CU} = \frac{\partial q_u(z) m_b}{\partial z} - \frac{\partial \tilde{q}(z) m_b}{\partial z} - \frac{\partial q_d(z) m_0}{\partial z} + \frac{\partial \tilde{q}(z) m_0}{\partial z}. \qquad (5.3.2.3.13)$$

Because of the simplicity of the static control, these equations can be further simplified to give

$$\left(\frac{\partial \tilde{h}(k)}{\partial t}\right)_{CU} = m_b \frac{\partial \tilde{h}(z)}{\partial z}(1-\epsilon) + m_b\left(\frac{\partial h_u(z)}{\partial z} - \epsilon \frac{\partial h_d(z)}{\partial z}\right) \qquad (5.3.2.3.14)$$

$$\left(\frac{\partial q(k)}{\partial t}\right)_{CU} = m_b \frac{\partial \tilde{q}(z)}{\partial z}(1-\epsilon) + m_b\left(\frac{\partial q_u(z)}{\partial z} - \epsilon \frac{\partial q_d(z)}{\partial z}\right). \qquad (5.3.2.3.15)$$

The rainfall is defined as

$$R \equiv I_1 m_b (1-\beta). \qquad (5.3.2.3.16)$$

The second term on the righthand sides of equations (5.2.2.3.14) and (5.2.2.3.15) are due to downdrafts and are zero above the downdraft originating level. Below the updraft-air originating level, the first term of the right-hand sides are zero and only downdrafts affect the larger-scale environment. All variables in the flux terms can be determined from the equations of the static control, except m_b.

Dynamic control

Because of the simplicity of the above equations, many closure assumptions can be used. The most simple closure is a Kuo-type assumption, which relates the rainfall rate to the moisture convergence. However, more applicable seems to be a stability closure. Again we have two choices. We could assume that the clouds will remove the available buoyant energy as in other mesoscale parameterizations, or that the clouds will stabilize the environment as fast as the larger-scale (or also sub-grid scale) destabilizes it, or even a mixture of both. Although both assumptions are easily implemented, we chose the closure which depends on the rate of destabilization. In this closure the change of the available buoyant energy due to convection offsets the changes due to other effects (larger-scale destabilization as well as sub-grid scale destabilization), yielding

$$\left(\frac{dABE}{dt}\right)_{OTH} = -\left(\frac{dABE}{dt}\right)_{CU}. \tag{5.3.2.3.17}$$

Next, the change due to the convection is normalized in terms of the mass flux to read

$$\left(\frac{dABE}{dt}\right)_{CU} \equiv m_b\left(\frac{dABE}{dt}\right)_{NCU}, \tag{5.3.2.3.18}$$

where subscript NCU denotes the change of the available buoyant energy due to a cloud normalized by the cloud-base mass flux. Equations (5.3.2.3.17) and (5.3.2.3.18) are used to calculate m_b.

The Procedure

This section describes in detail the procedure necessary to calculate the convective feedback. First, we will explain the very simplistic approach to calculate a normalized feedback, then we will describe how the closure assumption determines the mass flux.

Using the larger-scale temperature and moisture fields (T_0, q_0) at time t_0, $h_u(z), h_d(z), q_u(z), q_d(z)$ are simply arrived at (see equations (5.3.2.3.6)-(5.3.2.3.10). The first calculation is the determination of the integrals I_1 and I_2 (calculated as residuals using equations (5.3.2.3.8) and (5.3.2.3.9). The next step is then to estimate the convective changes per unit mass flux (before knowing the actual m_b's). This is done by estimating the net change of a thermodynamic variable α in a layer k by using

$$\frac{\Delta p(k)}{g}\delta(\tilde{\alpha}(k)) = (1-\epsilon)(\tilde{\alpha}(k-.5) - \tilde{\alpha}(k+.5)), \tag{5.3.2.3.19}$$

where $\Delta p(k)$ is defined by $\Delta p(k) = p(k+.5) - p(k-.5)$. This subsidence is an environmental compensatory mass flux due to the updraft and downdraft mass fluxes inside the cloud. Note that below z_u the "compensatory subsidence" may be compensatory uplifting, since in that case only downdrafts exist.

At the cloud top,

$$\frac{\Delta p(ktop)}{g}\delta(\tilde{\alpha}(ktop)) = -\tilde{\alpha}(ktop-.5) + \alpha_u(ktop). \tag{5.3.2.3.20}$$

Here $\Delta p(ktop) = p(ktop + .5) - p(ktop - .5)$. Finally, at the surface (the downdraft tops)

$$\frac{\Delta p(ksur)}{g}\delta(\tilde{\alpha}(ksur)) = -\epsilon(-\tilde{\alpha}(ksur - .5) + \alpha_d(ksur)), \tag{5.3.2.3.21}$$

with $\Delta p(ksur) = p(ksur + .5) - p(ksur - .5)$. Here, the first term is the compensatory environmental mass flux, and the second term is the detrainment of all downdraft air at the bottom. These normalized changes are also used in the calculation of the final feedback (after m_b is determined), which is simply given by

$$\left(\frac{\partial \alpha(k)}{\partial t}\right)_{CU} = \delta(\alpha(k))m_b. \tag{5.3.2.3.22}$$

To calculate the mass flux m_b, we define the buoyant energy which is available to a cloud (updraft and downdraft) as

$$\begin{aligned} ABE = &\sum_{k=LFC}^{k=ktop}\left[\frac{g}{c_p\, T(k-.5)} * \left(\frac{\tilde{h}(kb) - \tilde{h}^*(k-.5)}{1+\gamma(k-.5)}\right) * (z(k-1) - z(k))\right] \\ &+ \sum_{k=z_0}^{k=sur}\left[\frac{g}{c_p\, T(k-.5)} * \left(\frac{\tilde{h}(k0) - \tilde{h}^*(k-.5)}{1+\gamma(k-.5)}\right) * (z(k) - z(k-1))\right] \end{aligned}. \tag{5.3.2.3.23}$$

where γ is defined in equation (5.3.2.2.15). We can calculate ABE (similar to Lord 1982) for the unchanged environment as well as for the environment which has been modified by some arbitrary mass flux $m_b'\Delta t'$. Hence, we can write

$$NA = \left(\frac{dABE}{dt}\right)_{NCU} = \frac{ABE' - ABE}{m_b'\Delta t'}. \tag{5.3.2.3.24}$$

ABE are calculated using T_0 and q_0, while ABE' are calculated after modification of the thermodynamic variables by an arbitrary amount of mass flux, $m_b'\Delta t'$, where

$$\alpha'(k) = \alpha(k) + \delta(\alpha(k))m_b'\Delta t'. \tag{5.3.2.3.25}$$

For a closure which depends on the rate of destabilization, we have to calculate the change in the available buoyant energy due to large-scale or other subgrid-scale effects. We modify the thermodynamic fields with

$$\alpha``(k) = \alpha_0 + \left(\frac{\partial \alpha}{\partial t}\right)_{LS+SUBG}\Delta t, \tag{5.3.2.3.26}$$

where (5.3.2.3.26) is applied at every timestep Δt. These double prime quantities are then used to calculate the changes in the available buoyant energy due to "non-convective" effects. As a result, the equation for the mass flux becomes

$$m_b = \frac{ABE'' - ABE}{(ABE' - ABE)m_b'}. \qquad (5.3.2.3.27)$$

5.3.3 Parameterization of shallow convection

The shallow convection scheme is constructed to be able to serve two tasks. It parameterizes planetary boundary layer (PBL) forced shallow non-precipitating convection as well as mid-tropospheric shallow convection caused by other sub-grid scale effects (such as cloud top radiational cooling). The first might not be necessary when the parameterization is coupled to a higher order closure PBL scheme. It will transport moisture from inside the boundary layer into the layers just above the boundary layer. This is accomplished by emulating bubbles (forced by surface heat and moisture fluxes only, with strong lateral mixing) which rise without precipitation formation through the top of the boundary layer into the free atmosphere, where they then lose their buoyancy. Because of the strong lateral mixing, they usually do not rise more than 50-75 mb. The physics involved in describing the second kind of shallow convection is the same, except for the forcing.

To parameterize this type of convection we assume that a "convective element" can be characterized by a bubble which rises through several model layers. It is assumed to be forced by planetary boundary layer fluxes or radiational cooling tendencies. Some of the elements of this parameterization are based on an Arakawa-Schubert type scheme (section 5.3.2.2) and some are based on the simple one-cloud scheme described in section 5.3.2.3. However, the clouds (shallow "convective elements") are characterized by different properties. They usually have large mixing, are non-precipitating, and have no convective-scale downdrafts. They are forced by subgrid-scale processes only. The following description will be focused on differences from the previously described models. Since the sole purpose of this scheme is to represent "very" shallow convection, it is also constructed as a one-cloud scheme. Although it implicitly uses equations (5.3.2.2.1)-(5.3.2.2.4), considerable simplifications can be made by assuming strong lateral mixing (detrainment being equally as strong as entrainment). Equations (5.3.2.2.1) through (5.3.2.2.4) then read

$$\mu = 0, \tag{5.3.3.1}$$

$$\mu_e = \mu_d = \frac{.2}{r}, \tag{5.3.3.2}$$

and

$$\frac{\partial \alpha_c}{\partial z} = \frac{.2}{r}(\tilde{\alpha} - \alpha_c) + S_c, \tag{5.3.3.3}$$

where r in equation (5.3.3.2) is the radius of the element. The parameterization will be sensitive to the choice of r. For this type of convection we assume $r = 50m$. When assuming that no precipitation forms or evaporates, equations (5.3.3.1)-(5.3.3.3), together with initial conditions (5.3.2.2.25) and (5.3.2.2.26), form a simple set of equations to determine the properties of the convective element, if r is given. Without precipitation formation, S_c in equation (5.3.3.3) is zero. For the feedback, equations (5.3.2.2.32)-(5.3.2.2.34) simply become

$$FS_s(z) \equiv [s_c(z) - \bar{s}(z)]m_c, \tag{5.3.3.4}$$

$$FS_q(z) \equiv [q_c(z) - \bar{q}(z)]m_c, \tag{5.3.3.5}$$

$$FS_l(z) \equiv l(z)m_c = 0. \tag{5.3.3.6}$$

The only unknown in these equations is the mass flux. It is determined in the dynamic control, where we make use of the definition of the cloud work function (5.3.2.2.40) and simply impose

$$\left(\frac{dA(scl)}{dt}\right)_{CU} = -\left(\frac{dA(scl)}{dt}\right)_{SUBG}. \tag{5.3.3.7}$$

Note that since the cloud work function is independent of mass flux (mass flux is constant with height), equation (5.3.2.2.40) for cloud-type scl simplifies to

$$A(scl) = \int_{z_B}^{z_T} \frac{g}{C_pT(z)}\frac{1}{1+\gamma}(h_c(z) - \tilde{h}^*(z))dz. \tag{5.3.3.8}$$

Subscript CU refers to the effects due to convection, and $SUBG$ to effects due to sub-grid scale forcing. $A(scl)$ becomes simply the buoyancy which is available for that particular cloud scl. Therefore, physically, the change of the efficiency of kinetic energy generation due to cloud scl is directly proportional to the buoyancy generation by sub-grid scale forcing. To arrive at a useful closure, the term on the left hand side of equation (5.3.3.7) is normalized by the massflux to yield

$$m_c \left(\frac{dA(scl)}{dt} \right)_{NCU} = - \left(\frac{dA(scl)}{dt} \right)_{SUBG} . \tag{5.3.3.10}$$

Here, the subscript NCU now stands for the change of A due to a unit mass of cloud scl. The variables in equation (5.3.3.10) are known, except for m_c. After using (5.3.3.10) to calculate m_c, we can then calculate the feedback. Note that in equation (5.3.3.2), mc is not dependent on height, and is simply the cloud base mass flux. It should be noted here that the above described parameterization will greatly benefit from a high vertical resolution. In some instances it may be of use to allow the shallow convection scheme to be called several times in a column (stacked on top of each other), since different sub-grid-scale forcing mechanisms may act at the same time in one column, but at different levels.

5.4 Planetary boundary layer parameterizations

5.4.1 Surface-Energy equation

Over land, the surface temperature T_g is computed from a surface energy budget that is base on the "force-restore" method developed by Blackadar (Zhang and Anthes 1982). The budget equation is

$$C_g \frac{\partial T_g}{\partial t} = R_n - H_m - H_s - L_v E_s, \tag{5.4.1.1}$$

where C_g is the thermal capacity of the slab per unit area, R_n is the net radiation, H_m is the heat flow into the substrate, H_s is the sensible heat flux into the atmosphere, L_v is the latent heat of vaporization, and E_s is the surface moisture flux. Blackadar (1979) shows that the following formulation enables the amplitude and phase of the slab temperature to be identical to the surface temperature of a real soil layer of uniform thermal conductivity λ and heat capacity per unit volume C_s, with C_g related to these parameters and the angular velocity of the earth Ω by

$$C_g = .95 \left(\frac{\lambda C_s}{2\Omega} \right)^{1/2}. \tag{5.4.1.2}$$

The thermal capacity, C_g, is related to a parameter called the thermal inertia, χ, where χ is

$$\chi = (\lambda C_s)^{1/2}. \tag{5.4.1.3}$$

From (5.4.1.2) and (5.4.1.3),

$$C_g = 3.293 \times 10^6 \chi, \tag{5.4.1.4}$$

where χ $(cal\ cm^{-2} K^{-1} s^{\frac{1}{2}};\ 1\ cal = 4.18\ J)$ is specified in the model as a function of land-use characteristic (Appendix 4). The terms on the right hand side of (5.4.1.1) are described as follows:

5.4.1.1 Net radiative flux R_n

Radiation is the driving force of the diabatic planetary boundary layer (PBL) and is the most important component of the slab-energy budget.

$$R_n = Q_s + I_s \tag{5.4.1.5}$$

where Q_s and I_s are the net surface shortwave and longwave irradiances.

a. Clear Sky

For clear sky, the amount of solar radiation absorbed by the slab, including multiple reflection of short waves, is approximated as

$$Q_s = S_0(1 - A)\tau cos\psi, \tag{5.4.1.6}$$

where S_0 is the solar constant (1395.6 W m^{-2}), A is the albedo. ψ is the zenith angle, and τ is the short-wave transmissivity. The term $cos\psi$ is given by

$$cos\psi = sin\phi sin\delta + cos\phi cos\delta cos h_0, \tag{5.4.1.7}$$

where ϕ represents the latitude of the location, δ the solar declination, and h_0 the local hour angle of the sun (Sellers. 1974).

The short-wave transmissivity for multiple reflection (Benjamin 1983) is

$$\tau = \frac{\tau_a[\tau_s + (1 - \tau_s)(1 - b)]}{(1 - X_R A)}, \tag{5.4.1.8}$$

where τ_a is the absorption transmissivity, τ_s is the scattering transmissivity, b is the backscattering coefficient, and X_R is the multiple reflection factor

$$X_R = \tau_{ad}(1 - \tau_{sd})b_d, \tag{5.4.1.9}$$

where the subscript d denotes diffuse.

All the clear-air transmissivities ($\tau_a, \tau_s, \tau_{ad}, \tau_{sd}$) and backscattering coefficients (b and b_d) are determined as a function of path length and precipitable water from a look-up table from the Carlson and Boland (1978) radiative transfer model. Transmissivities are then adjusted for surface pressure as follows:

$$\tau = \frac{1 + (\tau' - 1)p_s}{1013.25}, \tag{5.4.1.10}$$

where τ' is the transmissivity from the look-up table (appendix 2) obtained by assuming the surface pressure is 1013.25mb, and p_s is the surface pressure at the location. The net longwave radiation, I_s, is equal to the sum of the outgoing ($I \uparrow$) and downward ($I \downarrow$) longwave radiation. The outgoing longwave radiation is

$$I \uparrow = \epsilon_g \sigma_{SB} T_g^4, \tag{5.4.1.11}$$

where ϵ_g is the slab emissivity, T_g is the ground temperature, and σ_{SB} the Stefan-Boltzmann constant. The downward longwave radiation absorbed at the surface is

$$I \downarrow = \epsilon_g \epsilon_a \sigma_{SB} T_a^4, \tag{5.4.1.12}$$

where T_a is the atmospheric temperature in the layer above the surface, and ϵ_a, the atmospheric longwave emissivity, is given by

$$\epsilon_a = .725 + .17 log_{10} w_p, \tag{5.4.1.13}$$

in which w_p is the precipitable water in centimeters

b. Cloudy skies

For cloudy skies, a cloud parameterization scheme (Benjamin 1983) is used to simulate the effects of clouds on short-wave and downward longwave radiation. Groups of sigma levels are chosen to correspond to low-, middle-, and upper-cloud layers based upon an assumed surface pressure of 1000mb. The clouds below 800mb are designated as low clouds, middle clouds are those between 800mb and 450mb, and upper clouds are those above 450mb.

The attenuation of short-wave radiation by cloud is parameterized with absorption (τ_{ac}) and scattering (τ_{sc}) transmissivities. The transmissivities through the three cloud layers are given by

$$\tau_{ac} = \prod_{i=1}^{3} [1 - (1 - \tau_{ai})] n_i \tag{5.4.1.14}$$

and

$$\tau_{sc} = \prod_{i=1}^{3} [1 - (1 - \tau_{si})] n_i, \tag{5.4.1.15}$$

where $i = 1, 2, 3$ represents low, middle, and high clouds, respectively, n_i is the cloud fraction, and τ_{ai} and τ_{si} are given in table 5.1. The minimum short-wave absorption transmissivity is set at 0.7, and the minimum scattering transmissivity is set at 0.44.

The cloud fraction is based on relative humidity. Cloud fraction at low and middle levels is

$$n = 4.0RH - 3.0, \tag{5.4.1.16}$$

and in the upper atmosphere

$$n = 42.5RH - 1.5, \tag{5.4.1.17}$$

where RH is the maximum relative humidity found in the model layers within the low, middle, or upper cloud layers. The expression for effective short-wave transmissivity under cloudy skies is

$$\tau = \frac{\tau_{ac}\tau_{sc}\tau_a[\tau_s + (1-\tau_s)(1-b)]}{(1-X_cA)}, \tag{5.4.1.18}$$

where the multiple reflection factor for cloudy skies (X_c) is defined as

$$X_c = \tau_{ad}\tau_{ac}(1-\tau_{sd}\tau_{sc})\bar{b}_d \tag{5.4.1.19}$$

in which $\bar{b}_d$, the mean backscattering coefficient, is

$$\bar{b}_d = \frac{b_d(1-\tau_{sd}) + (1-\tau_{sc})}{(1-\tau_{sd}) + (1-\tau_{sc})}. \tag{5.4.1.20}$$

The cloud enhancement of long-wave radiation incident on the ground is expressed as

$$I\downarrow' = I\downarrow\left(1 + \sum_{i=1}^{3} c_i n_i\right), \tag{5.4.1.21}$$

where c_i are the enhancement coefficients at different levels (table 5.2).

Table 5.1 Cloud absorption and scattering transmissivities.

Cloud Level	**Absorption** (τ_{ai})	**Scattering** (τ_{si})
Low	**0.80**	**0.48**
Middle	**0.85**	**0.60**
High	**0.98**	**0.80**

Table 5.2 Enhancement coefficients c_i on longwave radiation due to clouds.

Cloud Level	**Coefficient**
Low	**0.26**
Middle	**0.22**
High	**0.06**

5.4.1.2 Heat Flow into the Substrate H_m

The transfer of heat due to molecular conduction is calculated from the equation

$$H_m = K_m C_g (T_g - T_m), \tag{5.4.1.22}$$

where K_m is the heat transfer coefficient expressed as $K_m = 1.18\Omega$, Ω is the angular velocity of the earth, and T_m is the temperature of the substrate, which is presently taken to be a constant value equal to the mean surface-air temperature over the period of simulation. If the model is used in a forecast mode rather than a research mode, T_m may be set equal to the mean surface temperature of the previous day.

5.4.1.3 Sensible-Heat Flux H_s and Surface Moisture Flux E_s

These fluxes are computed in different ways, depending upon what PBL parameterization is used. Details will be described in the next sections.

5.4.2 Bulk-aerodynamic parameterization

The bulk-aerodynamic option of the PBL physics follows Deardorff (1972). It is a very inexpensive choice. The surface-heat fluxes are given by

$$H_s = \rho_a c_{pm} C_\theta C_u (\theta_g - \theta_a) V, \tag{5.4.2.1}$$

where ρ_a and θ_a are density and potential temperature at the lowest model layer, C_θ and C_u are exchange coefficients (Deardorff 1972) defined as

$$C_u = C_{uN} \left(\frac{1 - R_{iB}}{R_{iC}} \right) \tag{5.4.2.2}$$

and

$$C_\theta = C_{\theta N} \left(\frac{1 - R_{iB}}{R_{iC}} \right) \tag{5.4.2.3}$$

for stable conditions ($0 \leq R_{iB} \leq .9 R_{ic}$), and

$$C_u = \frac{1}{\frac{1}{C_{uN}} - 25 exp(.26\psi - .03\psi^2)} \tag{5.4.2.4}$$

and

$$C_\theta = \frac{1}{\frac{1}{C_{\theta N}} + \frac{1}{C_u} - \frac{1}{C_{uN}}} \tag{5.4.2.5}$$

for the unstable case ($R_{iB} \leq 0$). Here C_{uN} and $C_{\theta N}$ are the neutral values for C_u and C_θ, and are given by

$$C_{uN} = \left[k^{-1} ln\left(\frac{.025h}{z_0}\right) + 8.4\right]^{-1} \tag{5.4.2.6}$$

and

$$C_{\theta N} = \left[0.74k^{-1} ln\left(\frac{.025h}{z_0}\right) + 7.3\right]^{-1}, \tag{5.4.2.7}$$

where $R_{ic} = 3.05$, h is the depth of the lowest model layer, ψ is defined as

$$\psi = log_{10}(-R_{iB}) - 3.5, \tag{5.4.2.8}$$

and the velocity V is given by

$$V = (V_a^2 + V_c^2)^{1/2}. \tag{5.4.2.9}$$

V_a is the wind-speed at the lowest model layer, and V_c is a convective velocity, which is important under conditions of low mean wind-speed and is defined under unstable and neutral conditions as

$$V_c = 2(\theta_g - \theta_a)^{1/2}, \tag{5.4.2.10}$$

while it is zero under stable conditions.

The surface moisture flux is

$$E_s = \rho_a C_\theta C_u M(q_{vs}(T_g) - q_{va})V, \tag{5.4.2.11}$$

where M is the moisture availability parameter which varies from 1.0 for a wet surface to 0.0 for a surface with no potential for evaporation. The moisture availability is specified as a function of land-use category (Appendix 4). The model results are often quite sensitive to the value used for M.

The surface momentum flux is given by

$$\tau_s = \rho_a C_D V^2, \tag{5.4.2.12}$$

where the drag coefficient C_D is defined as

$$C_D = C'_D + 3 \times 10^{-3}\left(\frac{\phi_s}{\phi_s + 9800}\right). \tag{5.4.2.13}$$

The second term in (5.4.2.13), involving the surface geopotential ϕ_s, is a correction for elevated terrain (Bleck,1977). The expression for C'_D follows Deardorff (1972), where

$$C'_D = C_u^2 \tag{5.4.2.14}$$

5.4.3 Blackadar High-resolution model

A revised version of Blackadar's PBL model (Blackadar, 1976, 1979; Zhang and Anthes, 1982) is used to forecast the vertical mixing of horizontal wind (u and v), potential temperature (θ), mixing ratio (q_v), cloud water (q_c), and ice (q_i). The surface heat and moisture fluxes are computed from similarity theory. First the friction velocity, u_*, is computed based on

$$u_* = MAX\left(\frac{kV}{ln\frac{z_a}{z_0} - \psi_m}, u_{*0}\right), \tag{5.4.3.1}$$

where u_{*0} is a background value ($0.1ms^{-1}$ over land and zero over water) and V is given by (5.4.2.9). The surface-heat flux is computed from

$$H_s = -C_{pm}\rho_a k u_* T_*, \tag{5.4.3.2}$$

where

$$T_* = \frac{\theta_a - \theta_g}{ln\frac{z_a}{z_0} - \psi_h}, \tag{5.4.3.3}$$

where z_0 is the roughness parameter, z_a is the height of the lowest σ-level, and ψ_m and ψ_h are nondimensional stability parameters that are a function of the bulk Richardson number R_{iB}, which is given by

$$R_{iB} = \frac{gz_a}{\theta_a}\frac{\theta_{va} - \theta_{vg}}{V^2}, \tag{5.4.3.4}$$

where the subscript v represents virtual potential temperature. There are four cases possible:

a. Stable case

For the stable case, $R_{iB} > R_{ic}$, where the critical Richardson number R_ic is defined as

$$R_{ic} = .2. \tag{5.4.3.5}$$

In this case,

$$u_* = u_{*0}, \tag{5.4.3.6}$$

$$\psi_m = \psi_h = -10 ln \frac{z_a}{z_0}, \tag{5.4.3.7}$$

and

$$H_s = Max(-250\ W\ m^{-2}, -c_{pm}\rho_a k u_* T_*). \tag{5.4.3.8}$$

b. Mechanically driven turbulence

For this case $0 \le R_{iB} \le R_{ic}$, and we get

$$\psi_m = \psi_h = -5 \left(\frac{R_{iB}}{1.1 - 5R_{iB}} \right) ln \frac{z_a}{z_0}. \tag{5.4.3.9}$$

c. Unstable (forced convection)

Here $R_{iB} < 0$ and $\mid h/L \mid \le 1.5$, where the Monin-Obukhov length, L, is defined as

$$L = -\frac{c_{pm}\rho_a \theta_a u_*^3}{kgH_s} \tag{5.4.3.10}$$

and h is the height of the PBL. In this case, $\psi_m = \psi_h = 0$, and $z_a/L = R_{iB} ln \frac{z_a}{z_0}$.

d. Unstable (free convection)

Here $R_{iB} < 0$ and $\mid h/L \mid > 1.5$. In this case

$$\psi_h = -3.23 \left(\frac{z_a}{L}\right) - 1.99 \left(\frac{z_a}{L}\right)^2 - 0.474 \left(\frac{z_a}{L}\right)^3, \tag{5.4.3.11}$$

and

$$\psi_m = -1.86 \left(\frac{z_a}{L}\right) - 1.07 \left(\frac{z_a}{L}\right)^2 - 0.249 \left(\frac{z_a}{L}\right)^3. \tag{5.4.3.12}$$

where z_a/L is restricted to be no less than -2.0 in this approximation. For z_a/L equal to -2.0, $\psi_h = 2.29$, and $\psi_m = 1.43$.

In the general case, z_a/L is a function of ψ_m and (5.4.3.12) is an implicit equation requiring an iterative solution. To save time, we approximate z_a/L as an explicit function of R_{iB}, such that

$$\frac{z_a}{L} = R_{iB} ln \frac{z_a}{z_0}. \tag{5.4.3.13}$$

The above scheme ensures continuity of ψ_m for all values of R_{iB}. The formulation for the surface moisture flux in the multi-layer case was derived from Carlson and Boland (1978), where

$$E_s = M\rho_a I^{-1}(q_{vs}(T_g) - q_{va}), \tag{5.4.3.14}$$

and

$$I^{-1} = ku_* \left[ln \left(\frac{ku_* z_a}{K_a} + \frac{z_a}{z_l} \right) - \psi_h \right]^{-1}. \tag{5.4.3.15}$$

The quantity z_l is the depth of the molecular layer (0.01 m over land and z_0 over water) and K_a is a background molecular diffusivity equal to $2.4 \times 10^{-5} m^2 s^{-1}$.

Over land, the roughness length z_0 is specified as a function of land-use category (Appendix 4). Over water, z_0 is calculated as a function of friction velocity (Delsol *et al.* , 1971) such that

$$z_0 = 0.032 u_*^2 / g + z_{0c}, \tag{5.4.3.16}$$

where z_{0c} is a background value of $10^{-4} m$.

The Blackadar scheme considers two different PBL regimes, the nocturnal regime and the free-convection regime. The first three cases (stable, mechanically driven turbulence, and forced convection) are in the nocturnal regime, which is usually stable or at most marginally unstable.

Nocturnal Regime

The first-order closure approach is used to predict model variables. The ground stress is calculated from

$$\tau_s = \rho u_*^2, \tag{5.4.3.17}$$

where u_* is computed from (5.4.3.1). The components of τ_s in the x and y directions are

$$\tau_{sx} = \frac{u}{V_a} \tau_s \tag{5.4.3.18}$$

and

$$\tau_{sy} = \frac{v}{V_a} \tau_s, \tag{5.4.3.19}$$

where V_a is the wind speed at the lowest model level. For surface layer variables, the prognostic equations are

$$\frac{\partial \theta_a}{\partial t} = \frac{-(H_1 - H_s)}{(\rho_a c_{pm} z_1)}, \tag{5.4.3.20}$$

$$\frac{\partial q_{va}}{\partial t} = \frac{-(E_1 - E_s)}{(\rho_a z_1)}, \tag{5.4.3.21}$$

$$\frac{\partial u_a}{\partial t} = \frac{(\tau_{1x} - \tau_{sx})}{(\rho_a z_1)}, \tag{5.4.3.22}$$

$$\frac{\partial v_a}{\partial t} = \frac{(\tau_{1y} - \tau_{sy})}{(\rho_a z_1)}, \tag{5.4.3.23}$$

and

$$\frac{\partial q_{ca}}{\partial t} = \frac{-F_1}{(\rho_a z_1)}, \tag{5.4.3.24}$$

where H_s is the surface heat flux computed from (5.4.3.2), E_S is the surface moisture flux computed from (5.4.3.14), subscript a refers to surface layer variables, subscript 1 refers to the fluxes at the top of the surface layer (Fig. 5.4), and z_1 is the height of the lowest model layer. The fluxes at the full σ levels are computed from K-theory, as described in section (5.4.4). The prognostic variables above the surface layer are computed from K-theory and an implicit diffusion scheme (Richtmeyer, 1957; Zhang and Anthes, 1982).

Free-Convection Regime

During strong heating from below, large surface heat fluxes and a super- adiabatic layer occur in the lower troposphere. As the buoyant plumes of hot air rise under such unstable conditions, mixing of heat, momentum, and moisture take place at each level. The vertical mixing in this scheme is not determined by local gradients, but by the thermal structure of the whole mixed layer. In the Blackadar PBL model, the vertical mixing is visualized as taking place between the lowest layer and each layer in the mixed layer, instead of between adjacent layers as in K-theory.

In the surface layer, the prognostic variables are solved by the analytic solution

$$\alpha_a^{\tau+1} = \alpha_a^{\tau-1} + \left(\frac{F_s z_1}{\bar{m}h^2} - \frac{F_s}{\bar{m}h} + \frac{F_1}{\bar{m}h}\right) \times \left[exp\left(-\frac{\bar{m}h\Delta t}{z_1}\right) - 1\right] + \frac{F_s \Delta t}{h}, \tag{5.4.3.25}$$

where α represents any prognostic variable, F_s is the surface flux, F_1 is the flux at the top of the surface layer, h is the height of the PBL, Δt is the time-step, and the mixing coefficient is

$$\bar{m} = H_1 \left[\rho_a c_{pm}(1-\epsilon) \int_{z_1}^{h} \left[\theta_{va} - \theta_v(z')\right] dz'\right]^{-1}. \tag{5.4.3.26}$$

Here ϵ is the entrainment coefficient (0.2) and H_1 is the heat flux at the top of the surface layer computed by the Priestly equation

$$H_1 = \rho_a c_{pm} z_1 (\theta_{va} - \theta_{v_{1\frac{1}{2}}})^{\frac{3}{2}} \left(\frac{2g}{27\theta_{va}} \right)^{\frac{1}{2}} \frac{1}{z_1} \left[z_1^{-\frac{1}{3}} - (2z_{1\frac{1}{2}})^{-\frac{1}{3}} \right]^{-\frac{3}{2}}, \qquad (5.4.3.27)$$

where z_1 is the depth of the surface layer and the subscript $1\frac{1}{2}$ refers to the second prediction layer above the surface (Fig. 5.4).

For the variables above the surface layer, the prognostic equation is

$$\frac{\partial \alpha_i}{\partial t} = \bar{m}(\alpha_a - \alpha_i), \qquad \alpha = \theta, q_v, or\ q_c \qquad (5.4.3.28)$$

$$\frac{\partial \alpha_i}{\partial t} = w\bar{m}(\alpha_a - \alpha_i), \qquad \alpha = u, v. \qquad (5.4.3.29)$$

The variable w is a weighting function for reducing mixing near the top of the mixed layer, where

$$w = 1 - \frac{z}{h}. \qquad (5.4.3.30)$$

Care must be taken at the layer where the top of the mixed layer is located because the top of the mixed layer does not necessarily coincide with a model level.

5.4.4 Vertical diffusion

Above the mixed layer, K-theory is used to predict the vertical diffusion of the prognostic variables, such that

$$F_V \alpha = p^* \frac{\partial}{\partial z} K_z \frac{\partial \alpha}{\partial z}, \qquad (5.4.4.1)$$

where the eddy diffusivity, K_z, is a function of the local Richardson number R_i. Specifically,

$$K_z = K_{z0} + l^2\ S^{\frac{1}{2}}\ \frac{R_{ic} - R_i}{R_{ic}} \qquad \text{for } R_i < R_{ic} \qquad (5.4.4.2)$$

$$K_z = K_{z0}, \qquad \text{for } R_i \geq R_{ic} \qquad (5.4.4.3)$$

where $K_{z0} = 1\ m^2\ s^{-1}$, $l = 40\ m$, $and R_{ic}$ is a critical Richardson number which is a function of layer thickness (m) and is defined as

$$R_{ic} = .257\ \Delta z^{.175}. \qquad (5.4.4.4)$$

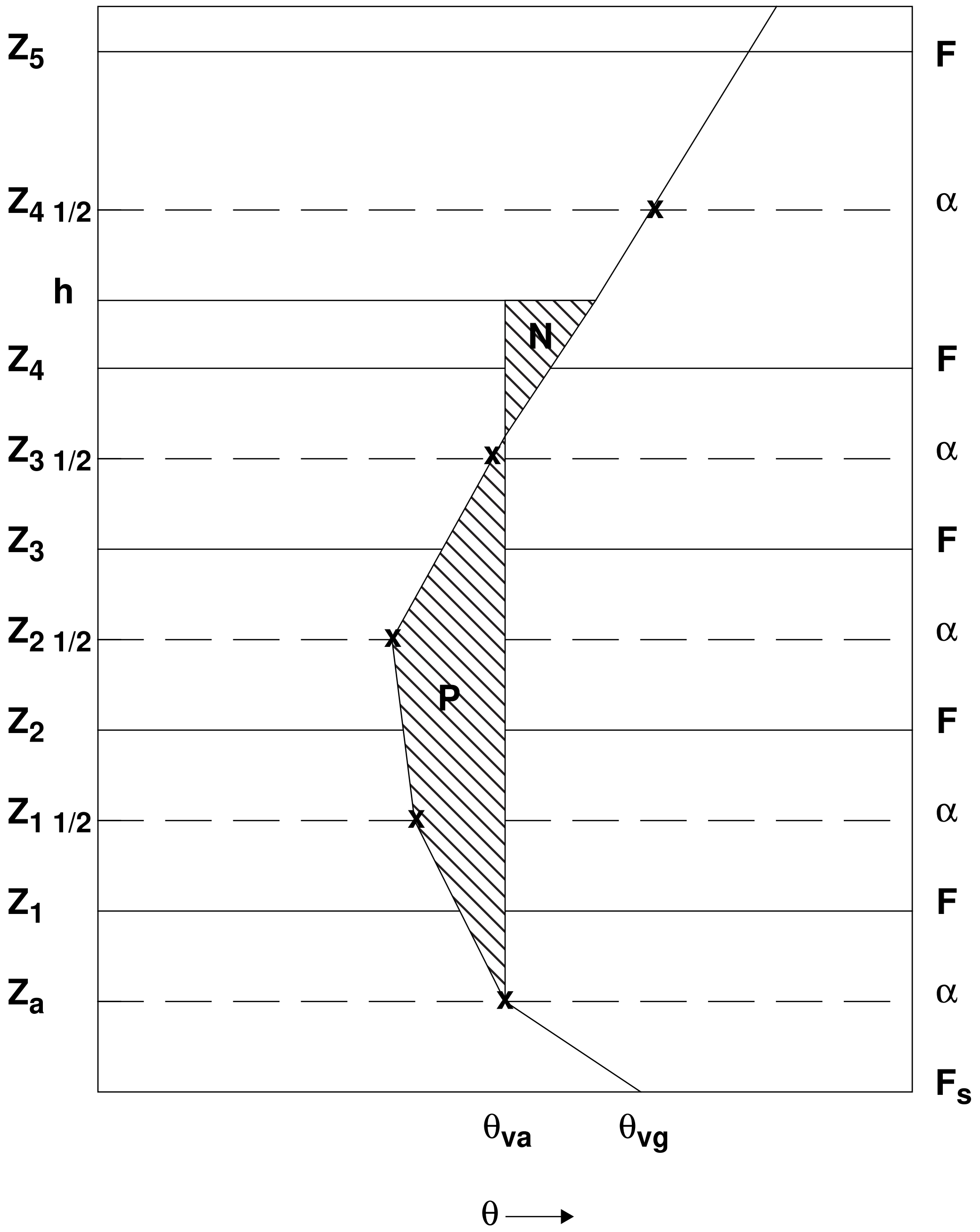

Figure 5.4 Illustration of vertical grid structure for high-resolution (Blackadar) model. The top of the surface layer is z_1; θ_{vg} and θ_{va} are the virtual potential temperatures of the ground surface and lowest model level, respectively; *P* and *N* denote the positive and negative areas associated with a parcel of air originating at z_a and rising to *h*, the top of the PBL.

According to (5.4.4.4), R_{ic} varies from 0.58 for $\Delta z = 100\,m$ to 0.86 for $\Delta z = 1000\,m$. The Richardson number is

$$R_i = \frac{g}{\theta S}\frac{\partial\theta}{\partial z} \tag{5.4.4.5}$$

and S is

$$S = \left(\frac{\partial u}{\partial z}\right)^2 + \left(\frac{\partial v}{\partial z}\right)^2 + 10^{-9}. \tag{5.4.4.6}$$

5.4.5 Moist vertical diffusion

There is an option with explicit moisture of including the effects of moisture on vertical diffusion. Taking into account moist-adiabatic processes in cloudy air (Durran and Klemp 1982), (5.4.4.5) is modified to

$$R_i = (1+\alpha)\left[\frac{g}{\theta S}\frac{\partial\theta}{\partial z} - \frac{g^2\frac{\chi-\alpha}{1+\chi}}{S c_p T}\right] \tag{5.4.5.1}$$

where

$$\chi = \frac{L_v^2 q_{vs}}{c_p R_v T^2} \tag{5.4.5.2}$$

and

$$\alpha = \frac{L_v q_{vs}}{R_d T}, \tag{5.4.5.3}$$

and this modified value is used in (5.4.4.2) where the cloud amount exceeds 0.01 g kg^{-1}.

5.5 Atmospheric radiation parameterization

The atmospheric radiation option in the model provides a longwave (infra-red) and shortwave (visible) scheme that interact with the atmosphere, cloud and precipitation fields, and with the surface (Dudhia 1989).

5.5.1 Longwave radiative scheme

Longwave absorption by water vapor, the primary clear-air absorber, is strongly spectral in character, and the method employed is the commonly used broadband emissivity method (see Stephens 1984). This involves using a precalculated emissivity function, ϵ, which represents the frequency-integrated absorption spectrum of water vapor, weighted by a suitable envelope function. Rodgers (1967) gives an upward and downward emissivity as a function of water vapor path, u, with a temperature correction term, where u includes a pressure correction factor proportional to $p^{0.86}$. The form of the fitted function is

$$\epsilon(u) = \sum_{i=0}^{i=4}(a_i + \overline{T}b_i)x^i, \qquad (5.5.1.1)$$

where $x = \ln u$ and $\overline{T}$ is a u-weighted T - 250K. For u less than 10 g m^{-2}, the form is

$$\epsilon(u) = \sum_{i=1}^{i=4}(c_i + \overline{T}d_i)y^i, \qquad (5.5.1.2)$$

where $y = u^{1/2}$ and a_i, b_i, c_i and d_i are constants. In the tropics, e-type absorption is an important additional component of the longwave absorption spectrum and is included with a similar fourth-order polynomial in ln (ue) to (5.5.1.1) from Stephens and Webster (1979), where e is the partial pressure due to water vapor. Given the emissivity functions from (5.5.1.1-2) (ϵ_u for upward flux and ϵ_d for downward flux), the upward and downward fluxes at any model level are given by

$$F_u = \int_0^1 B(T)d\epsilon_u, \qquad (5.5.1.3a)$$

$$F_d = \int_0^1 B(T)d\epsilon_d, \qquad (5.5.1.4a)$$

In (5.4.1.3a) the integration is performed downwards through the model layers. The quantity $d\epsilon$ is calculated for each layer using the temperature (T) of the layer and the frequency-integrated Planck function $B = \sigma_{SB}T^4$, where σ_{SB} is the Stefan-Boltzmann constant. When the surface is encountered, the ground emission F_{bot} is multiplied by $1-\epsilon$ and added to the integration. In (5.5.1.4a), the integration is performed upwards; the downward longwave flux at the model top, F_{top}, is assumed to result only from CO_2 emission in the stratosphere. Thus (5.5.1.3a-4a) can be expressed as

$$F_u(z) \;=\; \int_{z'=z}^{z'=z_{sfc}} B(T)\frac{d\epsilon_u}{dz'}dz' \;+\; F_{bot}[1-\epsilon_u(z,z_{sfc})], \tag{5.5.1.3b}$$

and

$$F_d(z) \;=\; \int_{z'=z}^{z'=z_{top}} B(T)\frac{d\epsilon_d}{dz'}dz' \;+\; F_{top}[(1-\epsilon_d(z,z_{top})], \tag{5.5.1.4b}$$

where

$$\epsilon(z,z_1) \;=\; \int_z^{z_1} \frac{d\epsilon}{dz'}dz'. \tag{5.5.1.5}$$

It can be seen from the formulas that if the emissivity reaches 1 during the integration, the remaining atmosphere makes no contribution to the flux. This is consistent with the idea that an emissivity of 1 corresponds to a "black" layer with respect to longwave radiation.

Following Stephens (1978), the cloud water is assumed to have a constant absorption coefficient which is slightly different for upward and downward radiation. The absorption coefficients are $\alpha_{cu} = 0.130$ m^2 g^{-1} and $\alpha_{cd} = 0.158$ m^2 g^{-1}. To combine these with water vapor absorption, the transmissivities are multiplied since clouds are assumed to be "grey bodies." The net emissivity is then

$$\epsilon_{tot} \;=\; 1 \;-\; T_v T_c, \tag{5.5.1.6}$$

with

$$T_v \;=\; 1 \;-\; \epsilon_{vapor} and \tag{5.5.1.7}$$

$$T_c \;=\; \exp(-\alpha_c u_c), \tag{5.5.1.8}$$

where u_c is the cloud water path (liquid mass per unit area).

Ice cloud is assumed to be composed of hexagonal plate-like crystals with the diameter-mass relation given in section (5.3.1.1). If the assumption is made that the crystals do not reflect longwave radiation and are sufficiently thick to be "black", it is possible to estimate an absorption coefficient as an integrated cross-sectional area. Allowing for the random orientation of these crystals and a hemispheric integration factor of 1.66, the absorption coefficient takes a value of $\alpha_i = 0.0735$ m^2 g^{-1}, or about half that of cloud water. Since this value agrees with some observations, it was applied in the model.

For rain and snow, the size distribution is necessary since the cross section is not proportional to the mass of a particle. The size spectrum changes with precipitation intensity so the absorption coefficient varies with precipitation amount. The effective absorption coefficient is given by

$$\alpha_p = \frac{1.66}{2000}\left(\frac{\pi N_0}{\rho_r^3}\right)^{1/4} \mathrm{m}^2\mathrm{g}^{-1}, \tag{5.5.1.9}$$

where ρ_r is the particle density. For the constants used in the explicit moisture scheme described earlier, the absorption coefficients take values of $2.34 \times 10^{-3}\mathrm{m}^2\mathrm{g}^{-1}$ for snow and $0.330 \times 10^{-3}\mathrm{m}^2\mathrm{g}^{-1}$ for rain. The effective water path for a layer of Δz meters thickness is given by

$$u_p = (\rho q_r)^{3/4}\Delta z \times 1000\mathrm{gm}^{-2}, \tag{5.5.1.10}$$

so that the transmissivity is given by

$$T_p = \exp(-\alpha_p u_p). \tag{5.5.1.11}$$

This transmissivity is multiplied with the others in (5.5.1.6) to give ϵ_{tot}. This is known as an overlap approximation. Rain and snow have less effect on the longwave flux by 2 to 3 orders of magnitude, but still are not insignificant.

Carbon dioxide is less easily treated since it cannot be assumed "grey". That is, its absorption is concentrated in a band of infrared wavelengths. To include its effect, an overlap method is used as discussed by Stephens (1984). In effect, the spectrum is divided into a carbon-dioxide band and a non-carbon-dioxide region. The former requires overlapping of the carbon dioxide transmissivity function while the latter does not. The relative weights of these two regions is slightly temperature dependent, but they add to give the total absorption. A pressure correction factor proportional to $p^{1.75}$ is applied to the carbon dioxide path calculation.

Having obtained the flux profiles, $F_u(z)$ and $F_d(z)$, the radiative heating rate is calculated from

$$\dot{Q}_R = c_p \frac{\partial T}{\partial t} = \frac{1}{\rho} \frac{\partial}{\partial z}(F_d - F_u) = -g \frac{\partial}{\partial p}(F_d - F_u). \tag{5.5.1.12}$$

In the model, the values of F are defined on the model full sigma-levels. This makes the various integrals and derivatives easier to represent numerically.

5.5.2 Shortwave Radiative Scheme

The downward component of shortwave flux is evaluated taking into account 1) the effects of solar zenith angle, which influences the downward component and the path length; 2) clouds, which have an albedo and absorption; 3) and clear air, where there is scattering and water-vapor absorption. Thus,

$$S_d(z) = \mu S_0 - \int_z^{top} (dS_{cs} + dS_{ca} + dS_s + dS_a), \tag{5.5.2.13}$$

where μ is the cosine of the zenith angle and S_0 is the solar constant.

As with the longwave scheme, cloud fraction in a grid box is either 0 or 1 because of the assumed stratiform nature of the clouds. The cloud back-scattering (or albedo) and absorption are bilinearly interpolated from tabulated functions of μ and $\ln(w/\mu)$ (where w is the vertically integrated cloud water path) derived from Stephens' (1978) theoretical results. The total effect of a cloud or multiple layers of cloud above a height z is found from the above function as a percentage of the downward solar flux absorbed or reflected. Then at a height $z - \Delta z$, a new total percentage is calculated from the table allowing the effect of the layer Δz to be estimated. However, this percentage is only applied to $\mu S_0 - \Delta S(clear\ air)$; that is, the clear-air effect above z is removed.

Clear-air water vapor absorption is calculated as a function of water vapor path allowing for solar zenith angle. The absorption function is from Lacis and Hansen (1974). The method is a similar integration-difference scheme to that described above for cloud.

Clear-air scattering is taken to be uniform and proportional to the atmosphere's mass path length, again allowing for the zenith angle, with a constant giving 20 percent scattering in one atmosphere. The heating rate is then given by

$$R_T = R_T(longwave) + \frac{1}{\rho c_p} S_{abs}, \tag{5.5.2.14}$$

where S_{abs} is defined from the absorption part of the S_d integral given in (5.5.2.13), since only cloud and clear-air absorption contribute to solar heating.

The solar and infrared fluxes at the surface, calculated from the atmospheric radiative schemes, are use in the energy budget of the land surface.